

TRUNCATED STELLAR DISCS IN X-RAY RICH ENVIRONMENTS

TRUNCATED STELLAR DISCS IN X-RAY RICH ENVIRONMENTS

By

MELANIE L. DEMERS, B.SC.

A Thesis

Submitted to the School of Graduate Studies

in Partial Fulfilment of the Requirements

for the Degree

Master of Science

McMaster University

©Copyright by Melanie Demers, September 2018

MASTER OF SCIENCE (2018)
(Physics and Astronomy)

McMaster University
Hamilton, Ontario

TITLE: Truncated Stellar Discs in X-ray Rich Environments

AUTHOR: Melanie Demers, B.Sc. (York University)

SUPERVISORS: Laura Parker

NUMBER OF PAGES: x, 98

Abstract

We study the dependence of galaxy disc components on environment using a sample of Sloan Digital Sky Survey Data Release 7 galaxies with structural parameters obtained via bulge-disc decompositions. We define two group environments based on X-ray richness at fixed halo mass, with an X-ray rich group sample and an X-ray poor group sample, and compare disc properties of galaxies in these environments to an isolated field population. At low bulge mass, we find evidence for galaxy stellar disc truncation in X-ray rich groups compared to both galaxies in X-ray poor groups and in the isolated field. Additionally, we show that galaxies in X-ray rich groups have smaller disc-to-total mass ratios than their isolated field counterparts. We find that our results are largely independent of group-centric position and halo mass; with the exception that disc truncation is slightly enhanced near the centres of large halos. Our findings demonstrate that galaxy stellar disc properties are sensitive to the X-ray brightness of their host group, more-so than local density parameters, suggesting that IGM-dependent hydrodynamic processes play a role in disc truncation. We suggest that ram-pressure stripping or starvation could be the mechanisms responsible for these results.

Acknowledgements

It is my belief that the proudest achievements are only made possible by standing on the shoulders of a strong community. Thankfully, the years leading up to this degree were built on a community of outstanding people.

To my supervisor, Laura Parker, thank you for your mentorship and candour. You enthusiastically shared your love of science with me, guided me to develop new ideas and ways of thinking, and were patient and supportive of my learning process.

To my committee members, Alison Sills and James Wadsley, thank you for providing a supportive learning environment with your unique teaching styles, and for your helpful comments on my research.

To my parents, thank you for your continued pride in me, for listening to me ramble about galaxies, and for the 500 km moves. To my sister Sarah Demers, thank you for being a lifelong source of laughter, rants, and blunt wisdom.

To my officemates and fellow graduate students – old and new – particularly Fraser Evans and Jasper Grond: thank you for coffee in the mornings, for wiggly arm dances, for beating me at crib, for shooting the Queen, for the breakfasts and beers, and for the advice on both science and life questions.

Thank you to my FNHMA family – Marion Crowe and Nicole Callihoo – for your strong mentorship, for teaching me to “pay it forward” and for your encouragement to combine modern astronomy with Indigenous teachings. To the SPPI DGO team – particularly Mary-Luisa Kapelus, Philippe Houle, Sylvie Charron, and Emily Gagnon – for encouraging me to speak my mind and to trust my gut more often.

Thank you to old friends: Natasha Zaveda for your wit, your sincerity, and your persistent optimism in every situation. To Leigh Stewart, for inspiring me with your perspective, and through the ardent pursuit of your dreams (life in the van). To Natalee Galati, my astro-cat, for so many giddy nights finishing assignments and colouring with sass. To Jackie Slomovic, for adjacent snuggles and cheesy bread in the lair. To Larysa Korbabicz, for your motivational phone calls and lively visits.

To Meghan Miholics, my sassiest best friend: for feeding me so often, for reminding me to take care of myself, and for giving me a fresh point of view on so many Democracy dates. You are the person I related to instantly when I first moved here, and your tenacity has helped shape me as a person. Taking spontaneous roadtrips and heading to the beach with you have been some of my favourite days.

To Paolo Bianchini, my “colleague”, “item”, and yoga partner-in-crime: for your amazing lunch-time gossip sessions, curry and cappuccinos, and aesthetic choices of seating. Your patio has become a peaceful safehaven for me, and I’m so glad someone else believes in bus-erology. You are one of the most mystical people I’ve ever met, and not only because you’re “learning English”. T’es ma poutine.

To Johnson Liang, my dingbat extraordinaire: for simultaneously motivating and infuriating me with perpetual humour, with philosophical questions, and with your laid-back ways. You have made me so much congee and tea I don’t even know where to begin. Thank you for your semi-brutal honesty, for making me laugh until I can’t see, and for your visceral compassion. You helped me see my own reflection.

To Selina Twum, my favourite dancer whose kindness was a reflex: I will honour your memory every day for the rest of my life, because you taught me what it means to uplift your community. This year especially, I’ve had a lot of “motivate-me cake” with you in mind. I miss you dearly, and aspire to exude the kind of love and positivity you graced the world with.

Merci infiniment à tous.

In loving memory of Selina Twum
01·06·1994 – 10·05·2017

Table of Contents

Descriptive Notes	ii
Abstract	iii
Acknowledgements	iv
List of Figures	ix
Co-Authorship	xi
Chapter 1 Introduction	1
1.1 Galaxy Properties	2
1.1.1 Colour	2
1.1.2 Star-formation Rate	4
1.1.3 Stellar Mass	5
1.1.4 Morphology	6
1.2 Galaxy Environment	9
1.2.1 Field	10
1.2.2 Groups and Clusters	11
1.3 Morphology and Environment	12
1.3.1 Mass-size Relation	15
1.4 Outline of this Thesis	16
Chapter 2 Truncated Stellar Discs in X-ray Rich Environments	33
Abstract	34
2.1 Introduction	35

2.2	Data	38
2.2.1	Group Properties	39
2.2.2	Galaxy Properties	41
2.2.3	Final Catalogues	45
2.3	Results	46
2.3.1	Trends with Stellar Mass	46
2.3.2	Disc Properties at Fixed Bulge Mass	49
2.3.3	Trends with Environmental Density	52
2.4	Discussion	56
2.4.1	Challenges with Galaxy Size Measurements	56
2.4.2	X-Ray Extreme Environments	57
2.4.3	Star-forming and Quiescent Discs	57
2.4.4	Trends by Morphological Type	59
2.4.5	Putting it all Together	61
2.5	Conclusions	64
Chapter 3 Further Observations of Disc Dependence on Environment		78
Chapter 4 Summary & Future Work		86

List of Figures

1.1	Sloan galaxies with $g - r$ colours	3
1.2	Sérsic index vs. stellar mass in varied bins of halo mass for group sample	15
1.3	Bulge-to-total mass ratio vs. stellar mass in varied bins of halo mass for group sample	15
2.1	Group X-ray luminosity vs. halo mass for entire group sample . .	43
2.2	Halo mass distributions for X-ray strong and X-ray weak systems	44
2.3	Mass-size relation for X-ray strong (XRS), X-ray weak (XRW) and field samples	48
2.4	Exponential disc scale length vs. stellar mass for XRS, XRW and field samples	50
2.5	Disc-to-total mass ratio vs. stellar mass for XRS, XRW and field samples	51
2.6	Exponential disc scale length vs. bulge mass for XRS, XRW and field samples	53
2.7	Disc-to-total mass ratio vs. bulge mass for XRS, XRW and field samples	54
2.8	Exponential disc scale length vs. bulge mass for XRS, XRW and field samples in bins of halo mass and group-centric radius . .	55
2.9	Exponential disc scale length vs. bulge mass for X-ray extremes (ex-XRS and ex-XRW) and field sample	58
2.10	Exponential disc scale length vs. bulge mass for star-forming galaxies	60

2.11	Exponential disc scale length vs. bulge mass divided by morphological type (Sa/Sb and Sc/Sd) for XRS, XRW and field samples	62
3.1	Exponential disc scale length vs. bulge mass for XRS, XRW and field samples with no applied V_{max} weights.	81
3.2	Exponential disc scale length vs. bulge mass for large halo masses, small halo masses, and in field sample	82
3.3	X-ray strength vs. halo mass for entire group sample	83
3.4	Exponential disc scale length vs. bulge mass as a function of X-ray strength	84
4.1	Optical image of an SDSS galaxy in the MaNGA survey	90
4.2	H α map created with MaNGA data	90

Co-Authorship

Chapter 2 of this thesis has been submitted to *Monthly Notices of the Royal Astronomical Society* (MNRAS). This work was co-authored by my supervisor Dr. Laura Parker. The third co-author, Ian Roberts, created the isolated field sample of galaxies used in this work. I hereby grant an irrevocable, non-exclusive license to McMaster University and Library Archives Canada to reproduce the material as part of this thesis.

Chapter 1

Introduction

Galaxies are the building blocks of the Universe, tracing out the large-scale baryonic structure of the Cosmic Web (see Fig. 1.1). For the past two decades, large-scale surveys such as the Sloan Digital Sky Survey (SDSS; York et al., 2000), the 2dF Galaxy Redshift Survey (2dFGRS; Colless et al., 2001), the Two Micron All Sky Survey (2MASS; Skrutskie et al., 2006) and the Cosmic Evolution Survey (COSMOS; Scoville et al., 2007) have used photometry (imaging in several broad wavelength bands) and spectroscopy (dispersed light as a function of wavelength) to measure galaxy properties. Using photometry, some of the properties we can measure include colour, photometric redshifts and galaxy morphology. With spectroscopy, we can determine spectroscopic redshifts (which are more accurate than photometric redshifts, and are a proxy for distance) as well as galaxy chemical composition. The wealth of observational data resulting from these photometric and spectroscopic surveys allows us to explore interdependencies between galaxy properties, and how galaxies vary in different environments.

From such surveys, we now know that galaxies in the local Universe generally follow a bi-modal distribution in colour (see §1.1.1), where the “red peak” generally corresponds to early-type galaxies, and the “blue peak” generally corresponds to late-type galaxies (e.g. Strateva et al., 2001; Blanton et al., 2003; Baldry et al., 2004; Balogh et al., 2004). It is generally thought that over time

actively star-forming late-type galaxies evolve into quiescent early-type galaxies through two channels: internal mechanisms that scale with galaxy stellar mass, and external mechanisms that quench (or shut off) star-formation (Peng et al., 2010). By comparing observations directly to galaxy simulations, we can develop a physical understanding of how galaxies evolve over cosmic time. In the rest of this chapter, we will provide a brief overview of galaxy properties (§1.1), galaxy environment (§1.2), and some of the physical mechanisms that are responsible for the transformation of galaxy properties with environment (§1.3).

1.1 Galaxy Properties

Galaxies are characterized by a wide range of observable properties. Through careful analysis of how these properties interrelate and how they depend on redshift, we can elucidate the mechanisms through which galaxies evolve into the populations we see today.

1.1.1 Colour

Galaxy colour is defined as the difference in magnitudes between two wavebands. For example, using the u , g , r , i , z photometric system with bands centered at 3590Å, 4810Å, 6230Å, 7640Å, 9060Å (see Fukugita et al., 1996), subtracting $u - g$, $g - r$, etc. magnitudes gives us a measurement of colour. Galaxies with low $g - r$ colours are bluer, while galaxies with high $g - r$ colours are redder.

Colour is a useful tool to explore galaxy evolution since it is easily measured. Moreover, since colour is a reflection of a galaxy's underlying stellar population, it can be used to characterize star-formation histories using models with minimal assumptions (e.g. Conroy et al., 2009, 2010; Conroy & Gunn,

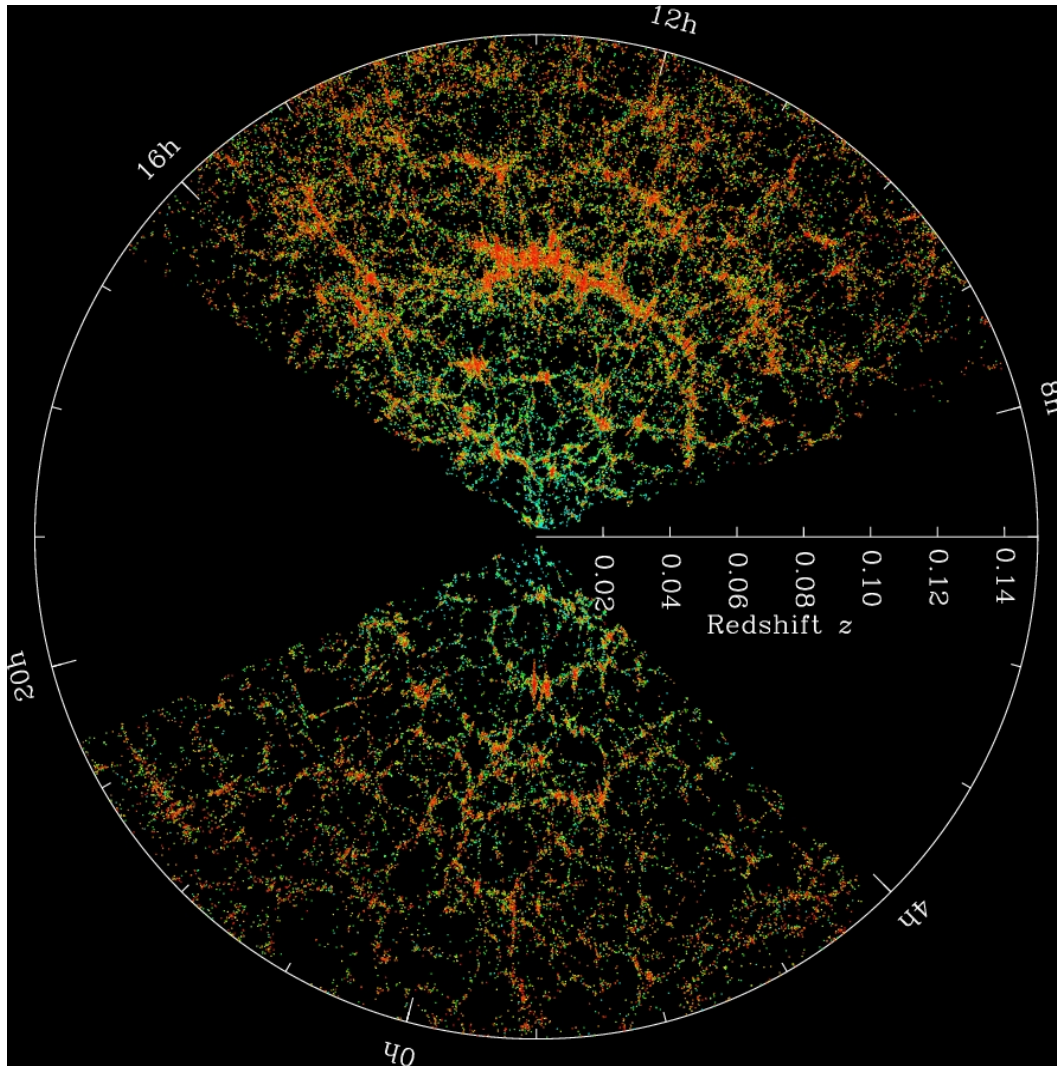


Figure 1.1 Map of the Universe displaying filamentary structure, where each dot is one galaxy. Colours correspond to Sloan $g - r$ definition (see §1.1.1). Image credit: M. Blanton and SDSS.

2010). Observations show that galaxy populations follow a bi-modal distribution in broadband colour (e.g. Strateva et al., 2001; Blanton et al., 2003) that is well-fit by a double Gaussian profile (Baldry et al., 2004; Balogh et al., 2004). These two populations are colloquially known as the “blue cloud” and “red sequence” of galaxies, with an intermediate sparsely populated region known as the “green valley”. It has been postulated that galaxies evolve from the blue cloud onto the red sequence through cosmic time (e.g. Peng et al., 2010; Trayford et al., 2016). Past works have shown that colour bi-modality holds out to at least $z \sim 2$ (e.g. Cassata et al., 2008).

1.1.2 Star-formation Rate

Star-formation rate (SFR) is a measure of the number of new stars forming in a galaxy in solar masses per year. It is an important galaxy property to measure, because declining star-formation rates are indicative of “quenching”, the process of shutting-off star-formation. SFR is more challenging to measure than colour, but there are a number of methods available.

SFR can be estimated from UV continuum emission. Since the UV continuum (1250–2500Å) is dominated by the stellar output of massive young stars, it is a tracer of recent star-formation in galaxies (Kennicutt, 1998; Hao et al., 2011). Although, one caveat with this method is that UV emission is heavily attenuated by the presence of dust. Another method that can be used is IR continuum emission (10 - 300 μm), which represents light from young stars that is absorbed and re-emitted by dust in thermal IR (Kennicutt, 1998). In particular, MIR emission at 15 μm and 24 μm is often used to trace star-formation (e.g. Koyama et al., 2008; Saintonge et al., 2008). IR continuum (thermal emission from dust-reprocessed light) can be measured in conjunction with UV continuum (emitted by massive young stars) to trace young star-formation and calculate how much light has been attenuated by dust. Moreover, using these

two measurements together can reduce statistical uncertainties compared to a single star-formation tracer (Kennicutt et al., 2009; Hao et al., 2011). Rather than continuum measurements, emission lines from ionized gas can also be used to measure SFR. The $H\alpha$ line is an example of a common recombination line used to measure SFR at local redshift, because it is a measure of re-processed ionized radiation from young stars and hence is an indicator of instantaneous star-formation (e.g. Glazebrook et al., 1999; Hirashita et al., 2003). Dust extinction is the primary source of error when using $H\alpha$ to measure SFRs (Kennicutt, 1998). At higher redshifts of $z \sim 1$, the strongest emission feature in the visible is the $[OII]\lambda 3727$ line (Kennicutt, 1998), and can be used to obtain star-formation rates of galaxies down to $\sim 0.3 M_{\odot} \text{yr}^{-1}$ (Gilbank et al., 2010).

Another SFR diagnostic is called the 4000\AA break, quantified by the $D_n(4000)$ index. When measuring the optical spectra of galaxies, populations of old stars produce absorption lines from ionized metals in their atmospheres, and this causes a break in their spectra at 4000\AA . Conversely, the elements in hot young stars become multiply ionized and this reduces opacity (weakening the break). A strong break is indicative of an old stellar population and a weak break is indicative of young stars (e.g. Hamilton, 1985; Brinchmann et al., 2004).

1.1.3 Stellar Mass

Galaxy stellar mass is an essential property to determine, because so many galaxy properties depend very strongly on it (Peng et al., 2010; Grützbauch et al., 2011, e.g.). The average colour of galaxies reddens with increasing stellar mass (van den Bosch et al., 2008), and the fraction of red galaxies increases with increasing stellar mass (Bamford et al., 2009; Prescott et al., 2011; Knobel et al., 2013). Moreover, quenched fractions of galaxies (fraction of galaxies with specific star-formation rates of $\text{SSFR} = \text{SFR}/M_{\star} < 10^{-11} \text{yr}^{-1}$) strongly

increase with increasing stellar mass (Wetzel et al., 2012). Morphology also becomes increasingly bulge-dominated with higher stellar masses, and depends on stellar mass more strongly than environment (e.g. Blanton et al., 2005; van der Wel et al., 2008; Bluck et al., 2014).

The primary method used to estimate stellar mass involves measuring a galaxy’s spectral energy distribution (SED), covering a wavelength range of UV, optical and NIR. The measured SED is compared to libraries of synthetic stellar populations, created using stellar population synthesis (SPS) codes (e.g. Bruzual & Charlot, 2003; Conroy et al., 2009, 2010; Conroy & Gunn, 2010). SPS codes have many input parameters such as stellar ages, metallicities, dust attenuation, and star-formation histories. To generate star-formation histories, a stellar initial mass function is adopted (e.g. Salpeter, 1955; Kroupa, 2002; Chabrier, 2003). Matching measured galaxy SEDs to the best fitting synthetic stellar population allows the estimation of galaxy parameters such as luminosity, star-formation rate and redshift, and leads to a measurement of stellar mass (e.g. Kauffmann et al., 2003; Mendel et al., 2014; Mobasher et al., 2015). Note that it is also possible to use spectral diagnostics such as the $D_n(4000)$ index to find the best fitting underlying stellar population, and hence measure stellar mass.

1.1.4 Morphology

1.1.4.1 Visual classification

Galaxies have been visually classified and identified since the early 1920s, upon the realization that “nebulae” were galaxies outside of our own (Hubble, 1926). Hubble generally categorized galaxies into elliptical (early-type), lenticular, spiral (late-type), and irregular by eye, and this classification system

has been in place until today (with some extensions by de Vaucouleurs, 1959; van den Bergh, 1960a,b, 1976). Briefly, elliptical galaxies are bulge-dominated, and labelled by an E followed by a number between 0 and 7 that denotes their degree of ellipticity, where E0 galaxies are circular and E7s are the most flattened. An intermediate class of galaxies called lenticulars, or S0 galaxies, have a central bulge-component with a disc, but no evidence of spiral patterns in their arms. Spiral galaxies have a central bulge with a disc component which has spiral structure. They are represented by an S followed by an a, b, c or d where a represents the most tightly wound arms, and d are fragmentary or loosely bound arms. If there is an elongated bar-like structure in the central bulge region of a spiral, these galaxies are denoted SB (meaning spiral bar), followed by a, b, c, d as well. Irregular galaxies are those with morphologies that do not match the three previous categories.

Although, Nair & Abraham (2010) emphasized the importance of visual inspection by experts, it is very labour intensive and it is not possible to visually classify entire modern surveys because the samples are so large. To handle these large samples, citizen science projects such as Galaxy Zoo and Galaxy Zoo 2 (see Lintott et al., 2008; Willett et al., 2013; Hart et al., 2016) can be used. These projects have allowed thousands of people to classify hundreds of thousands of galaxies. With large samples of public votes, visual identification by the public has proven to be as effective as professional astronomers, and agrees with their findings to an accuracy of better than 10 percent (Lintott et al., 2008).

1.1.4.2 Quantitative classification

There are several methods used to quantify morphology which reduce the subjectivity of visual classification and enable the classification of large samples. Trained experts are able to classify galaxies independently within two

Hubble types of each other (Naim et al., 1995). However, non-experts are not as reliable, unless there are thousands of participants classifying galaxies, which can be time-consuming. Visual classification also becomes challenging at higher redshifts, where substructure becomes increasingly difficult to resolve, making morphological type harder to determine.

The simplest method to quantify morphology is to use non-parametric measurements such as concentration (ratio of flux between an inner and outer isophote) and asymmetry (an indicator of the fraction of light in a galaxy’s non-symmetric components) (see Conselice, 2014, for a review). Non-parametric measurements are advantageous because they do not assume any underlying structure (as in parametric models), and they are reliable to redshifts of $z \sim 3$ (Conselice, 2003).

Parametric methods can also be used to provide a measure of morphology by fitting the optical surface brightness profiles of galaxies. Using a 1D model, Sérsic (1968) found that galaxies generally obey an exponentially declining surface brightness profile, written as follows:

$$\Sigma(r) = \Sigma_e \exp(-k[(r/R_e)^{1/n} - 1]) \quad (1.1)$$

where Σ_e is the surface brightness of the galaxy at effective radius R_e , n is the Sérsic index, and k is a normalization factor that depends on n . Many studies have shown that elliptical galaxies obey a de Vaucouleurs profile ($n = 4$) (de Vaucouleurs, 1948). It has also been shown that spiral galaxies generally have $n < 2.5$. The disc components of galaxies can generally be well-fit by $n = 1$ profiles (Freeman, 1970). More recently, 2D models have been developed to quantify morphology, treating bulges and discs separately. These simple 2D models can be achieved with two-component Sérsic fits, called bulge + disc decompositions (Peng et al., 2002; Simard et al., 2002, 2011). Bulge + disc decompositions do have limitations, including: the assumption that disc thick-

ness can be ignored, and the exclusion of parameters describing substructure or morphological disturbances of galaxies. Moreover, with noisy data it may not be possible to observe two distinct galaxy components.

1.1.4.3 Volume correction

It is important to note that most samples are not volume-limited, and therefore experience the Malmquist bias - a bias that allows high mass, high luminosity galaxies to be observed over large volumes, and only allows fainter, low mass galaxies to be observed over small, nearby volumes. To correct for the Malmquist bias, V_{max} weights can be applied, where V_{max} is the volume of the sample corresponding to the largest distance that a galaxy with a measurement of absolute magnitude can be observed in order to have an apparent magnitude equal to the magnitude limit of the sample. We use $1/V_{max}$ weights in our analysis from the Simard et al. (2011) catalogue by applying a weighted average to our galaxy parameters as follows:

$$\frac{\sum_{i=1}^N x_i \cdot 1/V_{max_i}}{\sum_{i=1}^N 1/V_{max_i}} \quad (1.2)$$

where x_i is an observed galaxy parameter x at i , and N is the total sample size.

1.2 Galaxy Environment

Galaxy evolution is influenced by the environment in which a galaxy lives. The term environment typically refers to the local density of a galaxy's surroundings. Some parameters commonly used to define environment in the literature are: group or cluster halo mass, projected nearest neighbour density (the surface density of galaxies in a sphere whose radius is equal to the pro-

jected distance to its n th nearest neighbour), and group-centric radius, among others (see Carollo et al., 2013, for a review). In this thesis, we will extend the latter definition of environment to include X-ray brightness within groups and clusters. Galaxy environment has been shown to affect many galaxy properties, such as star-formation rate, stellar mass, colour, and morphology (e.g. Dressler, 1980; Blanton et al., 2005; van der Wel et al., 2008; Balogh et al., 2007; Wilman et al., 2009; Bamford et al., 2009; Balogh et al., 2009; McGee et al., 2011; Wetzel et al., 2012). It is still debated whether morphology and colour evolve synchronously or separately. The evolution of colour and morphology could reflect two aspects of one evolutionary pathway, or be indicative of separate evolutionary mechanisms affecting galaxies differently (e.g. Ball et al., 2008; Skibba et al., 2009).

Additionally, any previous works that noted environmental trends were actually due to dependencies on stellar mass (Wetzel et al., 2012), because colour and SFR strongly correlate with stellar mass (e.g. Kauffmann et al., 2003) and massive galaxies are more commonly found in overdense environments (e.g. Hogg et al., 2003). To separate the dependence of galaxy properties on stellar mass (internal processes, referred to as “mass quenching”) and environment (external processes), many studies focus on trends with environment at fixed stellar mass. For more details on the effects of environment on morphology, see section §1.3.

1.2.1 Field

Galaxies that are in an isolated environment are known as field populations. The exact definition of field populations in the literature are quite varied. In this thesis, we use a strict catalogue of isolated field galaxies developed by Roberts & Parker (2017). Generally in field environments, galaxies are late-type and star-forming because environmental quenching mechanisms

are inefficient (e.g. Ball et al., 2008; Wetzel et al., 2012). Since isolated field galaxies are not influenced by intra-group medium (IGM hereafter) gas nor by other galaxies, they are useful when studying internal or secular evolutionary processes. For example, the effects of feedback from an active galactic nucleus (AGN) or bar can be ascertained more easily in field environments (Orban de Xivry et al., 2011; Fernández Lorenzo et al., 2012; Kocevski et al., 2012; Cheung et al., 2013).

1.2.2 Groups and Clusters

Groups of galaxies are the most common environments found in the low redshift Universe (Eke et al., 2004). Structure evolves hierarchically over time by accreting galaxies and other groups from the filaments of the Cosmic Web (e.g. McGee et al., 2009). They are interesting intermediate environments to study, because galaxies in groups display a wide range of morphologies (e.g. Zabludoff & Mulchaey, 2000) and bridge the gap between star-forming field galaxies and quiescent cluster galaxies. Studies have shown that the evolution of low mass galaxies in groups takes place much faster than in the field (Iovino et al., 2010; Kovač et al., 2010). Environmental mechanisms are effective in groups because the internal velocities of group member galaxies are similar to the groups' velocity dispersions, making galaxy-galaxy interactions more common than in clusters. Moreover, the presence of an IGM allows for galaxy-IGM quenching mechanisms to be more efficient than in the field (see §1.3).

Smaller groups are typically identified using optical spectroscopic selection methods (finding overdensities in redshift space). One such optical group-finding method is known as the Friends-of-friends (FOF) algorithm (e.g. Huchra & Geller, 1982; Davis et al., 1985). FOF algorithms can be applied to large datasets of galaxies, and apply strict criteria to define group membership based on short “linking lengths” in redshift space. Galaxies become linked if they have

smaller projected distances and differences in velocity than the chosen linking lengths. The FOF method is a popular way to define group membership, however if linking lengths are too large they can falsely link distinct groups together. Conversely, if linking lengths are too small the algorithm can incorrectly exclude member galaxies from groups (Jiang et al., 2014).

To address some of the challenges of traditional FOF algorithms, Yang et al. (2005) developed a halo-based group finder that refines group membership with additional phase-space information from halo-based parameters. In their method, it is assumed that the distribution of galaxies in phase-space follows that of dark matter particles in a spherical NFW profile (Navarro et al., 1997), and this acts as an added step to update group membership.

More massive groups and clusters can be identified using X-ray detections of the IGM or weak lensing, although X-ray detections may be biased towards systems with dense IGMs and not fully representative of the total population (Connelly et al., 2012). At higher redshifts, the cluster-red-sequence method can be used to identify galaxy clusters. Cluster elliptical galaxies are known to follow a red sequence in a colour-magnitude diagram (using an optical and a NIR filter). If an overdense region in space has an excess of early-type galaxies that fall on the cluster-red-sequence, it can be identified as a galaxy cluster (Gladders & Yee, 2000). Although, the cluster-red-sequence method is less effective for identifying groups that host galaxies with a range of colours.

1.3 Morphology and Environment

The fraction of galaxies with a given morphology correlates with environment, with bulge-dominated galaxies more commonly found in overdense environments and disc-dominated galaxies more commonly found in underdense environments (Oemler, 1974; Dressler, 1980; Postman & Geller, 1984; Dressler

et al., 1997; Lewis et al., 2002; Goto et al., 2003; Gómez et al., 2003; Balogh et al., 2004; Weinmann et al., 2006; Yang et al., 2007; Bamford et al., 2009); this is known as the morphology-density relation. Many of these early findings did not account for the strong dependence of morphology on stellar mass (as shown in Figs. 1.2 and 1.3, and by works such as van der Wel et al., 2008; Bamford et al., 2009; Bluck et al., 2014), combined with the fact that dense environments have more massive galaxies (e.g. Hogg et al., 2003). At fixed stellar mass, studies such as van den Bosch et al. (2008), Bamford et al. (2009) and Zhang & Yang (2017) show that galaxy morphology does weakly depend on environment (see Figs. 1.2 and 1.3). Taking stellar mass into account, the effect that environment has on different types of galaxies seems to be two-fold: for large bulge-dominated elliptical galaxies, morphology is independent of environment (Pohlen & Trujillo, 2006; Maltby et al., 2010; Maltby et al., 2015), while the structural parameters of low mass spiral galaxies are affected by environment (Tasca et al., 2009; Maltby et al., 2010; Zhang & Yang, 2017). Several mechanisms can be used to explain how galaxy structure could change with environment, and these environmental mechanisms fall into two general categories:

- Galaxy-galaxy interactions:
 - Major (two galaxies of comparable mass) and minor (one galaxy less massive than the other) mergers of galaxies, where major mergers are more rare in clusters than in groups, due to higher relative velocities (e.g. Toomre & Toomre, 1972; Cohn, 2012).
 - High-speed fly-bys of galaxies (harassment) and tidal interactions have been shown to structurally disturb disc morphologies (Moore et al., 1996; Cortese et al., 2006).

- Galaxy-IGM interactions:
 - Starvation (or strangulation) has two explanations: 1) a mechanism preventing cooling and accretion of hot halo gas onto galaxy discs 2) a mechanism that strips away the hot halo gas (the source of new gas eventually accreting onto the disc) via the IGM. Starvation causes the SFR in galaxy discs to decline on the timescale it takes the galaxy to consume its cold gas (Wetzell et al., 2012), and therefore may reduce the size of the stellar disc after star-formation stops (after $\gtrsim 2$ Gyr) (Larson et al., 1980; Bekki et al., 2002; Boselli et al., 2006; Moran et al., 2006; van den Bosch et al., 2008).
 - Ram-pressure stripping is a mechanism that removes atomic hydrogen and molecular gas from galaxy discs as a galaxy travels through the dense IGM (e.g. Gunn & Gott, 1972; Chung et al., 2007), and can strip galaxies of their gas over very fast timescales (~ 100 Myr) (Fujita & Nagashima, 1999; Quilis et al., 2000; Roediger & Hensler, 2005; Kapferer et al., 2009). Disc galaxies in clusters (with high IGM densities) are observed to have reduced ratios of gas/stellar scale lengths as compared to galaxies in the field (Bösch et al., 2013).

The IGM-dependent interactions listed above could be traced by X-ray emission in groups/clusters (emitted via thermal bremsstrahlung). There is some evidence in the literature that galaxies in X-ray bright groups contain more early-type galaxies than X-ray undetected groups (Zabludoff & Mulchaey, 1998). Additionally, Wang et al. (2014) find that there is a higher fraction of red (or quenched) galaxies in X-ray bright groups. These results are consistent with Roberts et al. (2016), who find that the star-forming fraction and disc fraction of galaxies in X-ray rich groups are lower than in X-ray poor groups. However, Poggianti et al. (2016) find that the number of galaxies

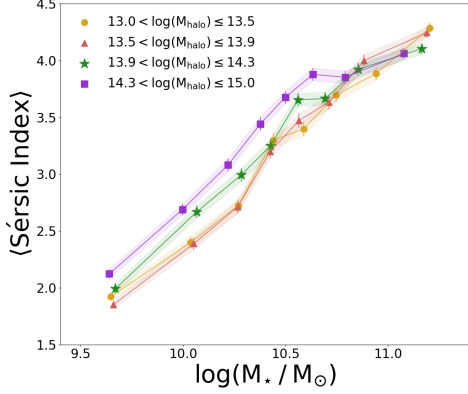


Figure 1.2 V_{max} weighted Sérsic index versus stellar mass in bins of halo mass as an indicator of environmental density, for our entire group sample described in §2.2.3.1. Error bars correspond to the standard error on the mean bin values, and are connected with shaded regions.

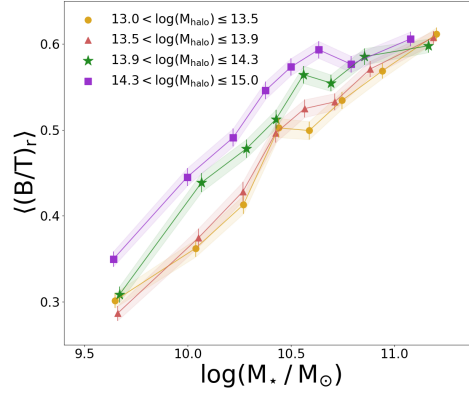


Figure 1.3 V_{max} weighted r band bulge-to-total mass ratio versus stellar mass in bins of halo mass, for our entire group sample described in §2.2.3.1. Error bars correspond to the standard error on the mean bin values, and are connected with shaded regions.

undergoing ram-pressure stripping (an IGM dependent process) in groups and clusters does not correlate with X-ray luminosity. We will further investigate the effects of X-ray brightness on galaxy structural parameters throughout Chapters 2 and 3.

1.3.1 Mass-size Relation

The relationship between galaxy mass and size is usually shown as the effective radius (or radius enclosing half of a galaxy’s light) versus stellar mass (e.g. Shen et al., 2003). The mass-size relation is a simple correlation that can be studied as a function of redshift and environment to trace how morphology evolves. The mass-size relation conveniently traces galaxy size at fixed stellar mass, which controls for mass dependent effects, and is a straightforward visualization of how galaxy sizes can grow or shrink. There are several challenges

in determining accurate galaxy size measurements, and these are summarized in section §2.4.1.

Several studies have shown that galaxy sizes (measured via effective radii) have grown from redshifts of ~ 3 until today (Daddi et al., 2005; Trujillo et al., 2006; Longhetti et al., 2007; Trujillo et al., 2007; Cimatti et al., 2008; van Dokkum et al., 2008). At constant stellar mass (above $10^{11} M_{\odot}$), this change in size can be characterized as a power law $R_e \propto \alpha(1+z)^{\beta}$, with a steeper slope for bulge-dominated galaxies ($\beta \sim -1.5$) than disc-dominated galaxies ($\beta \sim -0.8$) (Conselice, 2014). The differing power-law slopes indicate that bulge-dominated galaxies grew faster than disc-dominated galaxies over cosmic time.

At low redshift, the mass-size relation for early-type and lenticular galaxies has been shown to be independent of environment (Pohlen & Trujillo, 2006; Maltby et al., 2010; Maltby et al., 2015). However, environment does play a role in changing the mass-size relation for late-type spiral galaxies in the local Universe. Galaxy effective radii of low mass spirals in clusters are smaller than in the field (Tasca et al., 2009; Maltby et al., 2010), and this result may extend to higher mass spirals being affected by environment as well (Fernández Lorenzo et al., 2013). In contrast, Huertas-Company et al. (2013) show that the mass-size relation is independent of environment, from field to group halo mass range (with $\log(M_h/M_{\odot}) < 14$). We will investigate the dependence of the mass-size relation on X-ray brightness as a measure of environment in §2.3.1.1.

1.4 Outline of this Thesis

Broadly, the goal of this thesis is to address the question of whether galaxy morphology is affected by the X-ray richness of group environments, as com-

pared to the field. We are particularly interested in galaxy disc parameters for samples of galaxies with known bulge and disc properties (see Simard et al., 2011; Mendel et al., 2014), because we want to understand the extent to which stellar discs are affected by their local environment.

In Chapter 2, we probe how galaxy stellar discs respond to environment at fixed stellar mass and at fixed bulge mass. We specifically explore how disc scale length and disc-to-total mass ratio depend on group X-ray brightness as compared to an isolated field population. Chapter 2 represents the submitted version of *Truncated stellar discs in X-ray rich environments* to the *Monthly Notices of the Royal Astronomical Society*, a refereed astronomical journal. In Chapter 3, we investigate additional dependencies of disc scale length on environment. Lastly, Chapter 4 includes a summary of our results and ideas for future work.

Bibliography

- Baldry, I. K., Glazebrook, K., Brinkmann, J., Ivezić, Ž., Lupton, R. H., Nichol, R. C., & Szalay, A. S. 2004, *ApJ*, 600, 681
- Ball, N. M., Loveday, J., & Brunner, R. J. 2008, *MNRAS*, 383, 907
- Balogh, M. L., Baldry, I. K., Nichol, R., Miller, C., Bower, R., & Glazebrook, K. 2004, *ApJ*, 615, L101
- Balogh, M. L., McGee, S. L., Wilman, D., Bower, R. G., Hau, G., Morris, S. L., Mulchaey, J. S., Oemler, Jr., A., Parker, L., & Gwyn, S. 2009, *MNRAS*, 398, 754
- Balogh, M. L., Wilman, D., Henderson, R. D. E., Bower, R. G., Gilbank, D., Whitaker, R., Morris, S. L., Hau, G., Mulchaey, J. S., Oemler, A., & Carlberg, R. G. 2007, *MNRAS*, 374, 1169
- Bamford, S. P., Nichol, R. C., Baldry, I. K., Land, K., Lintott, C. J., Schawinski, K., Slosar, A., Szalay, A. S., Thomas, D., Tori, M., Andreescu, D., Edmondson, E. M., Miller, C. J., Murray, P., Raddick, M. J., & Vandenberg, J. 2009, *MNRAS*, 393, 1324
- Bekki, K., Couch, W. J., & Shioya, Y. 2002, *ApJ*, 577, 651
- Blanton, M. R., Eisenstein, D., Hogg, D. W., Schlegel, D. J., & Brinkmann, J. 2005, *ApJ*, 629, 143
- Blanton, M. R., Hogg, D. W., Bahcall, N. A., Brinkmann, J., Britton, M., Connolly, A. J., Csabai, I., Fukugita, M., Loveday, J., Meiksin, A., Munn, J. A., Nichol, R. C., Okamura, S., Quinn, T., Schneider, D. P., Shimasaku,

- K., Strauss, M. A., Tegmark, M., Vogeley, M. S., & Weinberg, D. H. 2003, *ApJ*, 592, 819
- Bluck, A. F. L., Mendel, J. T., Ellison, S. L., Moreno, J., Simard, L., Patton, D. R., & Starkenburg, E. 2014, *MNRAS*, 441, 599
- Bösch, B., Böhm, A., Wolf, C., Aragón-Salamanca, A., Barden, M., Gray, M. E., Ziegler, B. L., Schindler, S., & Balogh, M. 2013, *A&A*, 549, A142
- Boselli, A., Boissier, S., Cortese, L., Gil de Paz, A., Seibert, M., Madore, B. F., Buat, V., & Martin, D. C. 2006, *ApJ*, 651, 811
- Brinchmann, J., Charlot, S., White, S. D. M., Tremonti, C., Kauffmann, G., Heckman, T., & Brinkmann, J. 2004, *MNRAS*, 351, 1151
- Bruzual, G. & Charlot, S. 2003, *MNRAS*, 344, 1000
- Carollo, C. M., Cibinel, A., Lilly, S. J., Miniati, F., Norberg, P., Silverman, J. D., van Gorkom, J., Cameron, E., Finoguenov, A., Peng, Y., Pipino, A., & Rudick, C. S. 2013, *ApJ*, 776, 71
- Cassata, P., Cimatti, A., Kurk, J., Rodighiero, G., Pozzetti, L., Bolzonella, M., Daddi, E., Mignoli, M., Berta, S., Dickinson, M., Franceschini, A., Halliday, C., Renzini, A., Rosati, P., & Zamorani, G. 2008, *A&A*, 483, L39
- Chabrier, G. 2003, *PASP*, 115, 763
- Cheung, E., Athanassoula, E., Masters, K. L., Nichol, R. C., Bosma, A., Bell, E. F., Faber, S. M., Koo, D. C., Lintott, C., Melvin, T., Schawinski, K., Skibba, R. A., & Willett, K. W. 2013, *ApJ*, 779, 162
- Chung, A., van Gorkom, J. H., Kenney, J. D. P., & Vollmer, B. 2007, *ApJ*, 659, L115

Cimatti, A., Cassata, P., Pozzetti, L., Kurk, J., Mignoli, M., Renzini, A., Daddi, E., Bolzonella, M., Brusa, M., Rodighiero, G., Dickinson, M., Franceschini, A., Zamorani, G., Berta, S., Rosati, P., & Halliday, C. 2008, *A&A*, 482, 21

Cohn, J. D. 2012, *MNRAS*, 419, 1017

Colless, M., Dalton, G., Maddox, S., Sutherland, W., Norberg, P., Cole, S., Bland-Hawthorn, J., Bridges, T., Cannon, R., Collins, C., Couch, W., Cross, N., Deeley, K., De Propris, R., Driver, S. P., Efstathiou, G., Ellis, R. S., Frenk, C. S., Glazebrook, K., Jackson, C., Lahav, O., Lewis, I., Lumsden, S., Madgwick, D., Peacock, J. A., Peterson, B. A., Price, I., Seaborne, M., & Taylor, K. 2001, *MNRAS*, 328, 1039

Connelly, J. L., Wilman, D. J., Finoguenov, A., Hou, A., Mulchaey, J. S., McGee, S. L., Balogh, M. L., Parker, L. C., Saglia, R., Henderson, R. D. E., & Bower, R. G. 2012, *ApJ*, 756, 139

Conroy, C. & Gunn, J. E. 2010, *ApJ*, 712, 833

Conroy, C., Gunn, J. E., & White, M. 2009, *ApJ*, 699, 486

Conroy, C., White, M., & Gunn, J. E. 2010, *ApJ*, 708, 58

Conselice, C. J. 2003, *ApJS*, 147, 1

—. 2014, *ARA&A*, 52, 291

Cortese, L., Gavazzi, G., Boselli, A., Franzetti, P., Kennicutt, R. C., O’Neil, K., & Sakai, S. 2006, *A&A*, 453, 847

Daddi, E., Renzini, A., Pirzkal, N., Cimatti, A., Malhotra, S., Stiavelli, M., Xu, C., Pasquali, A., Rhoads, J. E., Brusa, M., di Serego Alighieri, S., Ferguson, H. C., Koekemoer, A. M., Moustakas, L. A., Panagia, N., & Windhorst, R. A. 2005, *ApJ*, 626, 680

Davis, M., Efstathiou, G., Frenk, C. S., & White, S. D. M. 1985, *ApJ*, 292, 371

de Vaucouleurs, G. 1948, *Annales d'Astrophysique*, 11, 247

—. 1959, *Handbuch der Physik*, 53, 275

Dressler, A. 1980, *ApJ*, 236, 351

Dressler, A., Oemler, Jr., A., Couch, W. J., Smail, I., Ellis, R. S., Barger, A., Butcher, H., Poggianti, B. M., & Sharples, R. M. 1997, *ApJ*, 490, 577

Eke, V. R., Baugh, C. M., Cole, S., Frenk, C. S., Norberg, P., Peacock, J. A., Baldry, I. K., Bland-Hawthorn, J., Bridges, T., Cannon, R., Colless, M., Collins, C., Couch, W., Dalton, G., de Propris, R., Driver, S. P., Efstathiou, G., Ellis, R. S., Glazebrook, K., Jackson, C., Lahav, O., Lewis, I., Lumsden, S., Maddox, S., Madgwick, D., Peterson, B. A., Sutherland, W., & Taylor, K. 2004, *MNRAS*, 348, 866

Fernández Lorenzo, M., Sulentic, J., Verdes-Montenegro, L., & Argudo-Fernández, M. 2013, *MNRAS*, 434, 325

Fernández Lorenzo, M., Sulentic, J., Verdes-Montenegro, L., Ruiz, J. E., Sabater, J., & Sánchez, S. 2012, *A&A*, 540, A47

Freeman, K. C. 1970, *ApJ*, 160, 811

Fujita, Y. & Nagashima, M. 1999, *ApJ*, 516, 619

Fukugita, M., Ichikawa, T., Gunn, J. E., Doi, M., Shimasaku, K., & Schneider, D. P. 1996, *AJ*, 111, 1748

Gilbank, D. G., Balogh, M. L., Glazebrook, K., Bower, R. G., Baldry, I. K., Davies, G. T., Hau, G. K. T., Li, I. H., & McCarthy, P. 2010, *MNRAS*, 405, 2419

- Gladders, M. D. & Yee, H. K. C. 2000, *AJ*, 120, 2148
- Glazebrook, K., Blake, C., Economou, F., Lilly, S., & Colless, M. 1999, *MNRAS*, 306, 843
- Gómez, P. L., Nichol, R. C., Miller, C. J., Balogh, M. L., Goto, T., Zabludoff, A. I., Romer, A. K., Bernardi, M., Sheth, R., Hopkins, A. M., Castander, F. J., Connolly, A. J., Schneider, D. P., Brinkmann, J., Lamb, D. Q., SubbaRao, M., & York, D. G. 2003, *ApJ*, 584, 210
- Goto, T., Yamauchi, C., Fujita, Y., Okamura, S., Sekiguchi, M., Smail, I., Bernardi, M., & Gomez, P. L. 2003, *MNRAS*, 346, 601
- Grützbauch, R., Conselice, C. J., Varela, J., Bundy, K., Cooper, M. C., Skibba, R., & Willmer, C. N. A. 2011, *MNRAS*, 411, 929
- Gunn, J. E. & Gott, III, J. R. 1972, *ApJ*, 176, 1
- Hamilton, D. 1985, *ApJ*, 297, 371
- Hao, C.-N., Kennicutt, R. C., Johnson, B. D., Calzetti, D., Dale, D. A., & Moustakas, J. 2011, *ApJ*, 741, 124
- Hart, R. E., Bamford, S. P., Willett, K. W., Masters, K. L., Cardamone, C., Lintott, C. J., Mackay, R. J., Nichol, R. C., Rosslowe, C. K., Simmons, B. D., & Smethurst, R. J. 2016, *MNRAS*, 461, 3663
- Hirashita, H., Buat, V., & Inoue, A. K. 2003, *A&A*, 410, 83
- Hogg, D. W., Blanton, M. R., Eisenstein, D. J., Gunn, J. E., Schlegel, D. J., Zehavi, I., Bahcall, N. A., Brinkmann, J., Csabai, I., Schneider, D. P., Weinberg, D. H., & York, D. G. 2003, *ApJ*, 585, L5
- Hubble, E. P. 1926, *ApJ*, 64
- Huchra, J. P. & Geller, M. J. 1982, *ApJ*, 257, 423

Huertas-Company, M., Mei, S., Shankar, F., Delaye, L., Raichoor, A., Covone, G., Finoguenov, A., Kneib, J. P., Le, F. O., & Povic, M. 2013, MNRAS, 428, 1715

Iovino, A., Cucciati, O., Scodreggio, M., Knobel, C., Kovač, K., Lilly, S., Bolzonella, M., Tasca, L. A. M., Zamorani, G., Zucca, E., Caputi, K., Pozzetti, L., Oesch, P., Lamareille, F., Halliday, C., Bardelli, S., Finoguenov, A., Guzzo, L., Kampczyk, P., Maier, C., Tanaka, M., Vergani, D., Carollo, C. M., Contini, T., Kneib, J.-P., Le Fèvre, O., Mainieri, V., Renzini, A., Bongiorno, A., Coppa, G., de la Torre, S., de Ravel, L., Franzetti, P., Garilli, B., Le Borgne, J.-F., Le Brun, V., Mignoli, M., Pellò, R., Peng, Y., Perez-Montero, E., Ricciardelli, E., Silverman, J. D., Tresse, L., Abbas, U., Bottini, D., Cappi, A., Cassata, P., Cimatti, A., Koekemoer, A. M., Leauthaud, A., Maccagni, D., Marinoni, C., McCracken, H. J., Memeo, P., Meneux, B., Porciani, C., Scaramella, R., Schiminovich, D., & Scoville, N. 2010, A&A, 509, A40

Jiang, L., Helly, J. C., Cole, S., & Frenk, C. S. 2014, MNRAS, 440, 2115

Kapferer, W., Sluka, C., Schindler, S., Ferrari, C., & Ziegler, B. 2009, A&A, 499, 87

Kauffmann, G., Heckman, T. M., White, S. D. M., Charlot, S., Tremonti, C., Brinchmann, J., Bruzual, G., Peng, E. W., Seibert, M., Bernardi, M., Blanton, M., Brinkmann, J., Castander, F., Csábai, I., Fukugita, M., Ivezić, Z., Munn, J. A., Nichol, R. C., Padmanabhan, N., Thakar, A. R., Weinberg, D. H., & York, D. 2003, MNRAS, 341, 33

Kennicutt, Jr., R. C. 1998, ARA&A, 36, 189

Kennicutt, Jr., R. C., Hao, C.-N., Calzetti, D., Moustakas, J., Dale, D. A., Bendo, G., Engelbracht, C. W., Johnson, B. D., & Lee, J. C. 2009, ApJ, 703, 1672

Knobel, C., Lilly, S. J., Kovač, K., Peng, Y., Bschorr, T. J., Carollo, C. M., Contini, T., Kneib, J.-P., Le Fevre, O., Mainieri, V., Renzini, A., Scoddeggio, M., Zamorani, G., Bardelli, S., Bolzonella, M., Bongiorno, A., Caputi, K., Cucciati, O., de la Torre, S., de Ravel, L., Franzetti, P., Garilli, B., Iovino, A., Kampczyk, P., Lamareille, F., Le Borgne, J.-F., Le Brun, V., Maier, C., Mignoli, M., Pello, R., Perez Montero, E., Presotto, V., Silverman, J., Tanaka, M., Tasca, L., Tresse, L., Vergani, D., Zucca, E., Barnes, L., Bordoloi, R., Cappi, A., Cimatti, A., Coppa, G., Koekemoer, A. M., López-Sanjuan, C., McCracken, H. J., Moresco, M., Nair, P., Pozzetti, L., & Welikala, N. 2013, *ApJ*, 769, 24

Kocevski, D. D., Faber, S. M., Mozena, M., Koekemoer, A. M., Nandra, K., Rangel, C., Laird, E. S., Brusa, M., Wuyts, S., Trump, J. R., Koo, D. C., Somerville, R. S., Bell, E. F., Lotz, J. M., Alexander, D. M., Bournaud, F., Conselice, C. J., Dahlen, T., Dekel, A., Donley, J. L., Dunlop, J. S., Finoguenov, A., Georgakakis, A., Giavalisco, M., Guo, Y., Grogin, N. A., Hathi, N. P., Juneau, S., Kartaltepe, J. S., Lucas, R. A., McGrath, E. J., McIntosh, D. H., Mobasher, B., Robaina, A. R., Rosario, D., Straughn, A. N., van der Wel, A., & Villforth, C. 2012, *ApJ*, 744, 148

Kovač, K., Lilly, S. J., Cucciati, O., Porciani, C., Iovino, A., Zamorani, G., Oesch, P., Bolzonella, M., Knobel, C., Finoguenov, A., Peng, Y., Carollo, C. M., Pozzetti, L., Caputi, K., Silverman, J. D., Tasca, L. A. M., Scoddeggio, M., Vergani, D., Scoville, N. Z., Capak, P., Contini, T., Kneib, J.-P., Le Fèvre, O., Mainieri, V., Renzini, A., Bardelli, S., Bongiorno, A., Coppa, G., de la Torre, S., de Ravel, L., Franzetti, P., Garilli, B., Guzzo, L., Kampczyk, P., Lamareille, F., Le Borgne, J.-F., Le Brun, V., Maier, C., Mignoli, M., Pello, R., Perez Montero, E., Ricciardelli, E., Tanaka, M., Tresse, L., Zucca, E., Abbas, U., Bottini, D., Cappi, A., Cassata, P., Cimatti, A., Fumana, M.,

- Koekemoer, A. M., Maccagni, D., Marinoni, C., McCracken, H. J., Memeo, P., Meneux, B., & Scaramella, R. 2010, *ApJ*, 708, 505
- Koyama, Y., Kodama, T., Shimasaku, K., Okamura, S., Tanaka, M., Lee, H. M., Im, M., Matsuhara, H., Takagi, T., Wada, T., & Oyabu, S. 2008, *MNRAS*, 391, 1758
- Kroupa, P. 2002, *Science*, 295, 82
- Larson, R. B., Tinsley, B. M., & Caldwell, C. N. 1980, *ApJ*, 237, 692
- Lewis, I., Balogh, M., De Propriis, R., Couch, W., Bower, R., Offer, A., Bland-Hawthorn, J., Baldry, I. K., Baugh, C., Bridges, T., Cannon, R., Cole, S., Colless, M., Collins, C., Cross, N., Dalton, G., Driver, S. P., Efstathiou, G., Ellis, R. S., Frenk, C. S., Glazebrook, K., Hawkins, E., Jackson, C., Lahav, O., Lumsden, S., Maddox, S., Madgwick, D., Norberg, P., Peacock, J. A., Percival, W., Peterson, B. A., Sutherland, W., & Taylor, K. 2002, *MNRAS*, 334, 673
- Lintott, C. J., Schawinski, K., Slosar, A., Land, K., Bamford, S., Thomas, D., Raddick, M. J., Nichol, R. C., Szalay, A., Andreescu, D., Murray, P., & Vandenberg, J. 2008, *MNRAS*, 389, 1179
- Longhetti, M., Saracco, P., Severgnini, P., Della Ceca, R., Mannucci, F., Bender, R., Drory, N., Feulner, G., & Hopp, U. 2007, *MNRAS*, 374, 614
- Maltby, D. T., Aragón-Salamanca, A., Gray, M. E., Barden, M., Häußler, B., Wolf, C., Peng, C. Y., Jahnke, K., McIntosh, D. H., Böhm, A., & van Kampen, E. 2010, *MNRAS*, 402, 282
- Maltby, D. T., Aragón-Salamanca, A., Gray, M. E., Hoyos, C., Wolf, C., Jogee, S., & Böhm, A. 2015, *Monthly Notices of the Royal Astronomical Society*, 447, 1506

McGee, S. L., Balogh, M. L., Bower, R. G., Font, A. S., & McCarthy, I. G. 2009, MNRAS, 400, 937

McGee, S. L., Balogh, M. L., Wilman, D. J., Bower, R. G., Mulchaey, J. S., Parker, L. C., & Oemler, A. 2011, MNRAS, 413, 996

Mendel, J. T., Simard, L., Palmer, M., Ellison, S. L., & Patton, D. R. 2014, ApJS, 210, 3

Mobasher, B., Dahlen, T., Ferguson, H. C., Acquaviva, V., Barro, G., Finkelstein, S. L., Fontana, A., Gruetzbauch, R., Johnson, S., Lu, Y., Papovich, C. J., Pforr, J., Salvato, M., Somerville, R. S., Wiklind, T., Wuyts, S., Ashby, M. L. N., Bell, E., Conselice, C. J., Dickinson, M. E., Faber, S. M., Fazio, G., Finlator, K., Galametz, A., Gawiser, E., Giavalisco, M., Grazian, A., Grogin, N. A., Guo, Y., Hathi, N., Kocevski, D., Koekemoer, A. M., Koo, D. C., Newman, J. A., Reddy, N., Santini, P., & Wechsler, R. H. 2015, ApJ, 808, 101

Moore, B., Katz, N., Lake, G., Dressler, A., & Oemler, A. 1996, Nature, 379, 613

Moran, S. M., Ellis, R. S., Treu, T., Salim, S., Rich, R. M., Smith, G. P., & Kneib, J.-P. 2006, ApJ, 641, L97

Naim, A., Lahav, O., Buta, R. J., Corwin, Jr., H. G., de Vaucouleurs, G., Dressler, A., Huchra, J. P., van den Bergh, S., Raychaudhury, S., Sodre, Jr., L., & Storrie-Lombardi, M. C. 1995, MNRAS, 274, 1107

Nair, P. B. & Abraham, R. G. 2010, ApJS, 186, 427

Navarro, J. F., Frenk, C. S., & White, S. D. M. 1997, ApJ, 490, 493

Oemler, Jr., A. 1974, ApJ, 194, 1

Orban de Xivry, G., Davies, R., Schartmann, M., Komossa, S., Marconi, A., Hicks, E., Engel, H., & Tacconi, L. 2011, MNRAS, 417, 2721

Peng, C. Y., Ho, L. C., Impey, C. D., & Rix, H.-W. 2002, AJ, 124, 266

Peng, Y.-j., Lilly, S. J., Kovač, K., Bolzonella, M., Pozzetti, L., Renzini, A., Zamorani, G., Ilbert, O., Knobel, C., Iovino, A., Maier, C., Cucciati, O., Tasca, L., Carollo, C. M., Silverman, J., Kampczyk, P., de Ravel, L., Sanders, D., Scoville, N., Contini, T., Mainieri, V., Scodreggio, M., Kneib, J.-P., Le Fèvre, O., Bardelli, S., Bongiorno, A., Caputi, K., Coppa, G., de la Torre, S., Franzetti, P., Garilli, B., Lamareille, F., Le Borgne, J.-F., Le Brun, V., Mignoli, M., Perez Montero, E., Pello, R., Ricciardelli, E., Tanaka, M., Tresse, L., Vergani, D., Welikala, N., Zucca, E., Oesch, P., Abbas, U., Barnes, L., Bordoloi, R., Bottini, D., Cappi, A., Cassata, P., Cimatti, A., Fumana, M., Hasinger, G., Koekemoer, A., Leauthaud, A., Maccagni, D., Marinoni, C., McCracken, H., Memeo, P., Meneux, B., Nair, P., Porciani, C., Presotto, V., & Scaramella, R. 2010, ApJ, 721, 193

Poggianti, B. M., Fasano, G., Omizzolo, A., Gullieuszik, M., Bettoni, D., Moretti, A., Paccagnella, A., Jaffé, Y. L., Vulcani, B., Fritz, J., Couch, W., & D'Onofrio, M. 2016, AJ, 151, 78

Pohlen, M. & Trujillo, I. 2006, A&A, 454, 759

Postman, M. & Geller, M. J. 1984, ApJ, 281, 95

Prescott, M., Baldry, I. K., James, P. A., Bamford, S. P., Bland-Hawthorn, J., Brough, S., Brown, M. J. I., Cameron, E., Conselice, C. J., Croom, S. M., Driver, S. P., Frenk, C. S., Gunawardhana, M., Hill, D. T., Hopkins, A. M., Jones, D. H., Kelvin, L. S., Kuijken, K., Liske, J., Loveday, J., Nichol, R. C., Norberg, P., Parkinson, H. R., Peacock, J. A., Phillipps, S., Pimblett, K. A., Popescu, C. C., Robotham, A. S. G., Sharp, R. G., Sutherland, W. J., Taylor,

- E. N., Tuffs, R. J., van Kampen, E., & Wijesinghe, D. 2011, MNRAS, 417, 1374
- Quilis, V., Moore, B., & Bower, R. 2000, Science, 288, 1617
- Roberts, I. D. & Parker, L. C. 2017, MNRAS, 467, 3268
- Roberts, I. D., Parker, L. C., & Karunakaran, A. 2016, MNRAS, 455, 3628
- Roediger, E. & Hensler, G. 2005, A&A, 433, 875
- Saintonge, A., Tran, K.-V. H., & Holden, B. P. 2008, ApJ, 685, L113
- Salpeter, E. E. 1955, ApJ, 121, 161
- Scoville, N., Aussel, H., Brusa, M., Capak, P., Carollo, C. M., Elvis, M., Gialalisco, M., Guzzo, L., Hasinger, G., Impey, C., Kneib, J.-P., LeFevre, O., Lilly, S. J., Mobasher, B., Renzini, A., Rich, R. M., Sanders, D. B., Schinnerer, E., Schminovich, D., Shopbell, P., Taniguchi, Y., & Tyson, N. D. 2007, ApJS, 172, 1
- Sérsic, J. L. 1968, Atlas de Galaxias Australes
- Shen, S., Mo, H. J., White, S. D. M., Blanton, M. R., Kauffmann, G., Voges, W., Brinkmann, J., & Csabai, I. 2003, MNRAS, 343, 978
- Simard, L., Mendel, J. T., Patton, D. R., Ellison, S. L., & McConnachie, A. W. 2011, ApJS, 196, 11
- Simard, L., Willmer, C. N. A., Vogt, N. P., Sarajedini, V. L., Phillips, A. C., Weiner, B. J., Koo, D. C., Im, M., Illingworth, G. D., & Faber, S. M. 2002, ApJS, 142, 1
- Skibba, R. A., Bamford, S. P., Nichol, R. C., Lintott, C. J., Andreescu, D., Edmondson, E. M., Murray, P., Raddick, M. J., Schawinski, K., Slosar, A., Szalay, A. S., Thomas, D., & Vandenberg, J. 2009, MNRAS, 399, 966

Skrutskie, M. F., Cutri, R. M., Stiening, R., Weinberg, M. D., Schneider, S., Carpenter, J. M., Beichman, C., Capps, R., Chester, T., Elias, J., Huchra, J., Liebert, J., Lonsdale, C., Monet, D. G., Price, S., Seitzer, P., Jarrett, T., Kirkpatrick, J. D., Gizis, J. E., Howard, E., Evans, T., Fowler, J., Fullmer, L., Hurt, R., Light, R., Kopan, E. L., Marsh, K. A., McCallon, H. L., Tam, R., Van Dyk, S., & Wheelock, S. 2006, *AJ*, 131, 1163

Strateva, I., Ivezić, Ž., Knapp, G. R., Narayanan, V. K., Strauss, M. A., Gunn, J. E., Lupton, R. H., Schlegel, D., Bahcall, N. A., Brinkmann, J., Brunner, R. J., Budavári, T., Csabai, I., Castander, F. J., Doi, M., Fukugita, M., Györy, Z., Hamabe, M., Hennessy, G., Ichikawa, T., Kunszt, P. Z., Lamb, D. Q., McKay, T. A., Okamura, S., Racusin, J., Sekiguchi, M., Schneider, D. P., Shimasaku, K., & York, D. 2001, *AJ*, 122, 1861

Tasca, L. A. M., Kneib, J.-P., Iovino, A., Le Fèvre, O., Kovač, K., Bolzonella, M., Lilly, S. J., Abraham, R. G., Cassata, P., Cucciati, O., Guzzo, L., Tresse, L., Zamorani, G., Capak, P., Garilli, B., Scodreggio, M., Sheth, K., Zucca, E., Carollo, C. M., Contini, T., Mainieri, V., Renzini, A., Bardelli, S., Bongiorno, A., Caputi, K., Coppa, G., de La Torre, S., de Ravel, L., Franzetti, P., Kampczyk, P., Knobel, C., Koekemoer, A. M., Lamareille, F., Le Borgne, J.-F., Le Brun, V., Maier, C., Mignoli, M., Pello, R., Peng, Y., Perez Montero, E., Ricciardelli, E., Silverman, J. D., Vergani, D., Tanaka, M., Abbas, U., Bottini, D., Cappi, A., Cimatti, A., Ilbert, O., Leauthaud, A., Maccagni, D., Marinoni, C., McCracken, H. J., Memeo, P., Meneux, B., Oesch, P., Porciani, C., Pozzetti, L., Scaramella, R., & Scarlata, C. 2009, *A&A*, 503, 379

Toomre, A. & Toomre, J. 1972, *ApJ*, 178, 623

Trayford, J. W., Theuns, T., Bower, R. G., Crain, R. A., Lagos, C. d. P., Schaller, M., & Schaye, J. 2016, *MNRAS*, 460, 3925

- Trujillo, I., Conselice, C. J., Bundy, K., Cooper, M. C., Eisenhardt, P., & Ellis, R. S. 2007, MNRAS, 382, 109
- Trujillo, I., Förster Schreiber, N. M., Rudnick, G., Barden, M., Franx, M., Rix, H.-W., Caldwell, J. A. R., McIntosh, D. H., Toft, S., Häussler, B., Zirm, A., van Dokkum, P. G., Labbé, I., Moorwood, A., Röttgering, H., van der Wel, A., van der Werf, P., & van Starkenburg, L. 2006, ApJ, 650, 18
- van den Bergh, S. 1960a, ApJ, 131, 558
- . 1960b, ApJ, 131, 215
- . 1976, ApJ, 206, 883
- van den Bosch, F. C., Aquino, D., Yang, X., Mo, H. J., Pasquali, A., McIntosh, D. H., Weinmann, S. M., & Kang, X. 2008, MNRAS, 387, 79
- van der Wel, A., Holden, B. P., Zirm, A. W., Franx, M., Rettura, A., Illingworth, G. D., & Ford, H. C. 2008, ApJ, 688, 48
- van Dokkum, P. G., Franx, M., Kriek, M., Holden, B., Illingworth, G. D., Magee, D., Bouwens, R., Marchesini, D., Quadri, R., Rudnick, G., Taylor, E. N., & Toft, S. 2008, ApJ, 677, L5
- Wang, L., Yang, X., Shen, S., Mo, H. J., van den Bosch, F. C., Luo, W., Wang, Y., Lau, E. T., Wang, Q. D., Kang, X., & Li, R. 2014, MNRAS, 439, 611
- Weinmann, S. M., van den Bosch, F. C., Yang, X., & Mo, H. J. 2006, MNRAS, 366, 2
- Wetzel, A. R., Tinker, J. L., & Conroy, C. 2012, MNRAS, 424, 232
- Willett, K. W., Lintott, C. J., Bamford, S. P., Masters, K. L., Simmons, B. D., Casteels, K. R. V., Edmondson, E. M., Fortson, L. F., Kaviraj, S., Keel, W. C., Melvin, T., Nichol, R. C., Raddick, M. J., Schawinski, K., Simpson, R. J., Skibba, R. A., Smith, A. M., & Thomas, D. 2013, MNRAS, 435, 2835

Wilman, D. J., Oemler, Jr., A., Mulchaey, J. S., McGee, S. L., Balogh, M. L., & Bower, R. G. 2009, *ApJ*, 692, 298

Yang, X., Mo, H. J., van den Bosch, F. C., & Jing, Y. P. 2005, *MNRAS*, 356, 1293

Yang, X., Mo, H. J., van den Bosch, F. C., Pasquali, A., Li, C., & Barden, M. 2007, *ApJ*, 671, 153

York, D. G., Adelman, J., John E. Anderson, J., Anderson, S. F., Annis, J., Bahcall, N. A., Bakken, J. A., Barkhouser, R., Bastian, S., Berman, E., Boroski, W. N., Bracker, S., Briegel, C., Briggs, J. W., Brinkmann, J., Brunner, R., Burles, S., Carey, L., Carr, M. A., Castander, F. J., Chen, B., Colestock, P. L., Connolly, A. J., Crocker, J. H., Csabai, I., Czarapata, P. C., Davis, J. E., Doi, M., Dombeck, T., Eisenstein, D., Ellman, N., Elms, B. R., Evans, M. L., Fan, X., Federwitz, G. R., Fiscelli, L., Friedman, S., Frieman, J. A., Fukugita, M., Gillespie, B., Gunn, J. E., Gurbani, V. K., de Haas, E., Haldeman, M., Harris, F. H., Hayes, J., Heckman, T. M., Hennessy, G. S., Hindsley, R. B., Holm, S., Holmgren, D. J., hao Huang, C., Hull, C., Husby, D., Ichikawa, S.-I., Ichikawa, T., Ivezić, Ž., Kent, S., Kim, R. S. J., Kinney, E., Klaene, M., Kleinman, A. N., Kleinman, S., Knapp, G. R., Korienek, J., Kron, R. G., Kunszt, P. Z., Lamb, D. Q., Lee, B., Leger, R. F., Limmongkol, S., Lindenmeyer, C., Long, D. C., Loomis, C., Loveday, J., Lucinio, R., Lupton, R. H., MacKinnon, B., Mannery, E. J., Mantsch, P. M., Margon, B., McGehee, P., McKay, T. A., Meiksin, A., Merelli, A., Monet, D. G., Munn, J. A., Narayanan, V. K., Nash, T., Neilsen, E., Neswold, R., Newberg, H. J., Nichol, R. C., Nicinski, T., Nonino, M., Okada, N., Okamura, S., Ostriker, J. P., Owen, R., Pauls, A. G., Peoples, J., Peterson, R. L., Petravick, D., Pier, J. R., Pope, A., Pordes, R., Prosapio, A., Rechenmacher, R., Quinn, T. R., Richards, G. T., Richmond, M. W., Rivetta, C. H., Rockosi, C. M., Ruthmansdorfer, K., Sandford, D., Schlegel, D. J., Schneider, D. P., Sekiguchi,

M., Sergey, G., Shimasaku, K., Siegmund, W. A., Smee, S., Smith, J. A., Snedden, S., Stone, R., Stoughton, C., Strauss, M. A., Stubbs, C., SubbaRao, M., Szalay, A. S., Szapudi, I., Szokoly, G. P., Thakar, A. R., Tremonti, C., Tucker, D. L., Uomoto, A., Berk, D. V., Vogeley, M. S., Waddell, P., Wang, S., Watanabe, M., Weinberg, D. H., Yanny, B., & Yasuda, N. 2000, *The Astronomical Journal*, 120, 1579

Zabludoff, A. I. & Mulchaey, J. S. 1998, *ApJ*, 496, 39

—. 2000, *ApJ*, 539, 136

Zhang, Y. & Yang, X. 2017, ArXiv e-prints

Chapter 2

Truncated Stellar Discs in X-ray Rich Environments

This chapter represents the scientific work, “*Truncated stellar discs in X-ray rich environments*” submitted to the refereed journal *Monthly Notices of the Royal Astronomical Society* by the following authors:

Melanie L. Demers, Laura C. Parker, Ian D. Roberts

Department of Physics & Astronomy, McMaster University

1280 Main Street West, Hamilton, ON, L8S 4L8, Canada

Abstract

We investigate the dependence of stellar disc properties on environment for a sample of Sloan Digital Sky Survey Data Release 7 galaxies with published photometric bulge-disc decompositions. We compare disc properties at fixed bulge mass for galaxies in an isolated field environment to galaxies in X-ray rich and X-ray poor groups. At low bulge mass, stellar discs in X-ray rich groups are significantly truncated compared to discs in both X-ray poor groups and in isolated field environments. Disc truncation is largely independent of group-centric position and halo mass, with the exception that disc truncation is mildly enhanced near the centres of large cluster-sized halos. We also find that stellar discs are truncated in X-ray rich environments for a subset of star-forming galaxies and for galaxies of different morphological types. Our results show that stellar disc properties depend on X-ray brightness, a tracer of IGM density, suggesting a role for hydrodynamic processes such as ram-pressure stripping and/or starvation.

2.1 Introduction

Galaxies in the local universe follow a largely bi-modal distribution in many observed properties (Brinchmann et al., 2004; Baldry et al., 2006; Driver et al., 2006; Bamford et al., 2009; Wetzel et al., 2012). In the star-formation rate (SFR) - stellar mass plane, these two populations of galaxies are separated into an actively star-forming “blue cloud” and a quiescent “red sequence” (e.g. Brinchmann et al., 2004). Blue cloud galaxies are typically disc-dominated and red sequence galaxies are often bulge-dominated. Previous work has suggested that galaxies evolve onto the red sequence through two distinct pathways: mass quenching and environmental quenching (e.g. Peng et al., 2010).

Environmental quenching is often used to explain the morphology-density relation, whereby red bulge-dominated galaxies are more likely to be found in dense environments, and blue disc-dominated galaxies are more commonly found in underdense environments (Oemler, 1974; Dressler, 1980; Lewis et al., 2002; Goto et al., 2003; Gómez et al., 2003; Balogh et al., 2004; Yang et al., 2007; Bamford et al., 2009). Although there are some exceptions to these trends - such as blue ellipticals (Schawinski et al., 2014) and red spirals (Masters et al., 2010; Evans et al., 2018) - the general bi-modality of galaxy colour and morphology holds true.

There are a host of environmental mechanisms invoked to explain the morphology-density relation. Galaxy mergers (both major and minor) have been proposed to explain the build-up of elliptical galaxies and the formation of bulges in the centres of spiral galaxies with time (e.g. Toomre & Toomre, 1972; Makino & Hut, 1997; Angulo et al., 2009; Wetzel et al., 2009a,b; White et al., 2010; Cohn, 2012). Other galaxy-galaxy interactions such as harassment and tidal encounters can also remove the gaseous and stellar discs of galaxies (Moore et al., 1996, 1998; Boselli et al., 2006; Cortese et al., 2006). These ef-

fects are more likely to occur in dense environments, although major mergers are rare in clusters due to high relative velocities (e.g. Conselice et al., 2009).

Galaxies also interact with the hot gas permeating group and cluster environments known as the intra-group or intra-cluster medium (IGM hereafter). Starvation (or strangulation), a process that prevents the cooling and accretion of hot halo gas onto galactic discs, or strips away hot halo gas via the IGM, is known to quench star-formation and can convert late-type spirals into early-type morphologies over long time scales (Larson et al., 1980; Bekki et al., 2002; van den Bosch et al., 2008). Based on observational results and simulations, it has been shown that starvation quenches star-formation on a timescale of $\gtrsim 1$ Gyr (Okamoto & Nagashima, 2003; Fujita, 2004; Tonnesen et al., 2007; Moran et al., 2007; Kawata & Mulchaey, 2008). Although, after star-formation stops, the gradual process of starvation preserves spiral structure for over ~ 1 Gyr before changes in morphology begin to take place (Bekki et al., 2002; Boselli et al., 2006; Moran et al., 2006). Since starvation is a slow-acting process, many observational studies at local redshift conclude that starvation only has a small affect on morphology (van den Bosch et al., 2008; Schawinski et al., 2014).

Ram-pressure stripping (e.g. Gunn & Gott, 1972) has also been observed to quench star-formation by removing atomic hydrogen gas from disc edges (e.g. Yagi et al., 2007; Zhang et al., 2013). In general, atomic hydrogen discs are more extended than stellar discs, and the stellar component is more tightly bound (e.g. Kennicutt, 1989). Since the atomic hydrogen disc is more loosely bound, the atomic hydrogen is more readily stripped than stars via processes such as ram-pressure stripping (Abadi et al., 1999; Joshi et al., 2017). This is consistent with observations showing that disc galaxies have reduced ratios of gas/stellar scale lengths in clusters as compared to field environments (Bösch et al., 2013). Models and simulations have shown that ram-pressure stripping can remove the entire gaseous component of discs in ~ 100 Myr in high den-

sity environments (Fujita & Nagashima, 1999; Quilis et al., 2000; Roediger & Hensler, 2005; Kapferer et al., 2009). Additionally, toy modelling of ram-pressure stripping studying the response of the stellar disc to the ram-pressure drag force on the gas disc has also shown that the *stellar disc* can be displaced by several kiloparsecs in the direction of the ram-pressure wind (Smith et al., 2012).

Environmental quenching mechanisms caused by the IGM, such as starvation and ram-pressure stripping, can possibly be traced by studying the X-ray luminosity of groups. For example, Zabludoff & Mulchaey (1998) find that X-ray bright groups (with the densest IGMs) have a higher fraction of early-type galaxies than X-ray undetected groups. However, not all studies find a dependence of morphology on X-ray environment. For example, Poggianti et al. (2016) find candidates for galaxies undergoing ram-pressure stripping in clusters and groups and these galaxies are found at all group-centric radii and their number does not correlate with X-ray host luminosity L_x .

The mass-size relation (e.g. Shen et al., 2003) is another useful tool for interpreting the growth of galaxies as a function of both redshift and of environment. Many studies have found that galaxy effective radii grow from redshifts 2-3 until today (Daddi et al., 2005; Trujillo et al., 2006; Longhetti et al., 2007; Trujillo et al., 2007; Cimatti et al., 2008; van Dokkum et al., 2008). To focus on environmental influences, previous studies have compared the mass-size relation at fixed redshift in different environments. At low (Pohlen & Trujillo, 2006; Maltby et al., 2010; Maltby et al., 2015) and high (Rettura et al., 2010; Valentinuzzi et al., 2010) redshift, studies have shown that the mass-size relation shows no environmental dependence for early-type and lenticular galaxies. However, Maltby et al. (2010) show that at low redshift, late-type spiral galaxies with $\log(M_*/M_\odot) < 10$ do depend on their environments, with effective radii that are $\sim 15 - 20\%$ larger in the field than in clusters. They conclude that environment can possibly play a role in reducing the sizes of

the discs of low mass spirals (in agreement with Tasca et al., 2009). Further, Fernández Lorenzo et al. (2013) showed that the discs of more massive spirals also display environmental dependencies.

Taking one step further, we can explore the effects of environment on bulges and discs separately. In order to study how the structural components of galaxies evolve with environment Driver et al. (2006) suggest modelling galaxies as two-component bulge + disc systems. There is an extensive body of literature that examines bulge scaling relations (e.g Magorrian et al., 1998; Marconi & Hunt, 2003; Häring & Rix, 2004; Graham, 2012, 2014; Bluck et al., 2014), and properties of spiral galaxies such as luminosity, rotational velocity, and disc size also obey known scaling relations (e.g. Courteau et al., 2007; Dutton et al., 2011). However, there is a relative lack of studies addressing the dependence of disc scaling relations on environment. If the bulges of low mass spiral galaxies have not experienced growth in stellar mass after $z \sim 1$ (van Dokkum et al., 2013), then galaxy discs continued to change with environment over cosmic time, and could drive overall changes in morphology (Hudson et al., 2010).

We analyze disc scale length and disc-to-total mass at fixed bulge mass in isolated field and group environments, using X-ray brightness as a proxy for the IGM density in groups. In §2.2, we describe our sample selection and data analysis. In §2.3, we present the disc scale length versus bulge mass relation for our sample. We discuss the implications of these results in §2.4 and present our conclusions in §2.5. This work assumes a Λ CDM cosmology with $\Omega_m = 0.3$, $\Omega_\Lambda = 0.7$, and $h = 0.7$.

2.2 Data

To examine the dependencies of galaxy discs on environment, we make use of a wealth of data from several public catalogues consisting of Sloan Digital

Sky Survey Data Release 7 (SDSS-DR7; Abazajian et al., 2009) galaxies and groups.

2.2.1 Group Properties

2.2.1.1 Group environment

We use a large sample of groups identified in SDSS-DR7 by Yang et al. (2007), hereafter Y07. The group finder developed by Yang et al. (2005, 2007) applies a modified Friends of Friends (FOF) algorithm (e.g Huchra & Geller, 1982; Davis et al., 1985) to the sample, and assigns galaxies to tentative groups based on short linking lengths in redshift-space. First, the FOF algorithm identifies tentative luminosity-weighted group centres. Next, Y07 calculate the characteristic luminosity of all assigned group members, such that the flux limit of the SDSS survey at different redshifts is taken into account. Subsequently, the group finder determines the halo mass of each tentative group, based on an assumed mass-to-light ratio and the luminosity of the group members. Using the halo mass, the halo radius and velocity dispersion are calculated for each group. Based on these halo parameters, Y07 adds or removes galaxies via their phase-space information to refine group membership. They repeat the latter steps iteratively until the assigned group membership remains unchanged (see Y07 for a complete description).

We calculate group-centric distances via the angular separation of each galaxy from the luminosity weighted centre of its host group following Hogg (1999). We normalize group-centric distances by the host group’s virial radius R_{200m} , calculated in Tinker & Chen (2008):

$$R_{200m} = \left(\frac{3M_{halo}}{4\pi \cdot 200\bar{\rho}_m} \right)^{1/3} \quad (2.1)$$

where M_{halo} is the group halo mass given in Y07, $\bar{\rho}_m = \Omega_{m,0} \rho_{c,0} (1 + z_g)^3$ is the average background matter density of the universe, and z_g is the redshift of the luminosity-weighted group centre. Using our assumed cosmology, this can be simplified to:

$$R_{200m} = 1.13h^{-1} \left(\frac{M_{halo}}{10^{14}h^{-1}M_{\odot}} \right)^{1/3} (1 + z_g)^{-1} \quad (2.2)$$

2.2.1.2 X-ray properties

We use group X-ray luminosities determined by Wang et al. (2014), who estimated the X-ray luminosities for 65,000 optically selected galaxy groups (and clusters) in the SDSS using X-ray data from the ROSAT All Sky Survey (RASS; Voges et al., 1999). Wang et al. (2014) use an Optical to X-ray (OTX) code (see Shen et al., 2008) to measure group X-ray luminosities. The OTX code begins with an optically identified group with $\log(M_{halo}/M_{\odot}) \gtrsim 13$ and identifies the most-massive galaxies (MMGs), keeping up to 4 MMGs for each group. Using a maximum likelihood algorithm, the RASS sources that are associated with the MMGs are identified, while masking out contaminant sources such as quasi-stellar objects and stars. The algorithm determines the X-ray background for each group by measuring the number of counts enclosed in a 6 arcminute wide annulus, whose inner ring corresponds to R_{200m} , that is centered on the X-ray centre. The X-ray background is subtracted off, and the cumulative source count rate profile as a function of radius is calculated for each group. Integrating the source count rate profile within $R_x = 0.5 R_{200m}$ results in an X-ray luminosity L_x for each group.

Wang et al. (2014) applies the OTX code to $\sim 65,000$ optical groups, and after background subtraction $\sim 34,500$ groups have signal-to-noise $S/N > 1$ in the X-ray. We limit our sample to galaxies with redshifts less than 0.1, so that our sample is relatively complete to $\log(M_*/M_\odot) \sim 9$. Our redshift cut reduces the group sample size by $\sim 50\%$. We also restrict halo masses (obtained from Y07) to be within $13 \leq \log(M_{\text{halo}}/M_\odot) \leq 15$, which results in a sample of ~ 4000 groups (as in Roberts et al., 2016).

2.2.2 Galaxy Properties

2.2.2.1 Structural parameters

We use bulge and disc decompositions of SDSS galaxies from Simard et al. (2011), hereafter S11. S11 uses the GIM2D software package (see Simard et al., 2002) to fit the two-dimensional surface brightness profiles of SDSS galaxies in the g and r bandpasses. There are three parametric models used for these fits: i) a fixed central bulge with a de Vaucouleurs profile $n_b = 4$ and a free disc ii) a free bulge and a free disc iii) a pure single-component Sérsic fit. In this work we use the structural parameters from a fixed de Vaucouleurs bulge and free disc (table 1 in S11). There are many structural parameters measured, but we specifically use the half-light radius and exponential disc scale length derived from the following expressions (Sérsic, 1968):

$$\Sigma(r) = \Sigma_e \exp(-k[(r/R_e)^{1/n} - 1]) \quad (2.3)$$

where Σ_e is the surface brightness of the galaxy at effective radius R_e , n is the Sérsic index, and $k = 1.9992n - 0.3271$ (Capaccioli, 1989). Elliptical galaxies and the classical bulges of spiral galaxies are well-described by a de Vaucouleurs

profile with $n = 4$. Galaxy discs have been shown to be well-fit by an $n = 1$ surface brightness profile (Andredakis et al. 1995; de Jong 1996; S11), such that:

$$\Sigma(r) = \Sigma_0 \exp(-r/R_d) \quad (2.4)$$

where Σ_0 is the central surface brightness of the galaxy, and R_d is the exponential disc scale length.

2.2.2.2 Bulge and disc properties

We obtain the total stellar, bulge, and disc masses from Mendel et al. (2014). The masses derived in the Mendel et al. (2014) catalogue are based on an extension of S11, with additional Sérsic decompositions of SDSS galaxies in the u , i and z bandpasses. To estimate stellar masses, each galaxy’s spectral energy distribution (SED) is compared to a library of synthetic stellar populations, generated by the stellar population synthesis (SPS) code developed and calibrated by Conroy et al. (2009, 2010) and Conroy & Gunn (2010). Each SPS library is constructed to incorporate a range of stellar ages, metallicities, star-formation histories, and dust parameters. There are two SPS libraries generated: i) one that accounts for internal dust attenuation in the SPS grid, following the extinction law of (Calzetti et al., 2000) ii) the other fixes $E(B-V) = 0$, and assumes a dust-free model. A Bayesian approach is used to carry out the SED fits for a given SPS library, where a likelihood function describing the flux of each object in the u , g , r , i , z bands is defined, and the priors are defined via the construction of the SPS grid. We use the dust-corrected stellar, bulge and disc mass estimates, but we find no differences in our results when using dust-free estimates.

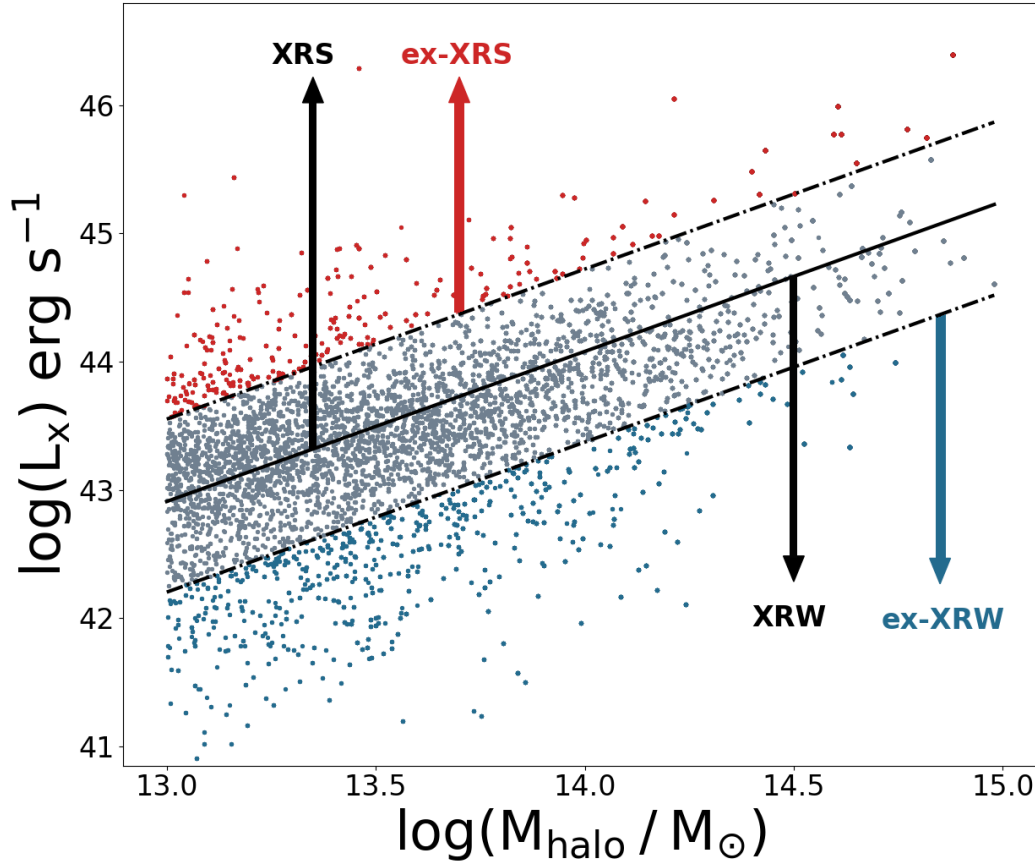


Figure 2.1 Galaxy group samples in the $L_x - M_{\text{halo}}$ plane. Groups above and below the solid line of best fit delineate the X-ray strong (XRS) and X-ray weak (XRW) group samples. The top (red) and bottom (blue) deciles of the dataset that lie above and below the dashed lines are referred to as the extremely X-ray strong (ex-XRS) and extremely X-ray weak (ex-XRW) group samples.

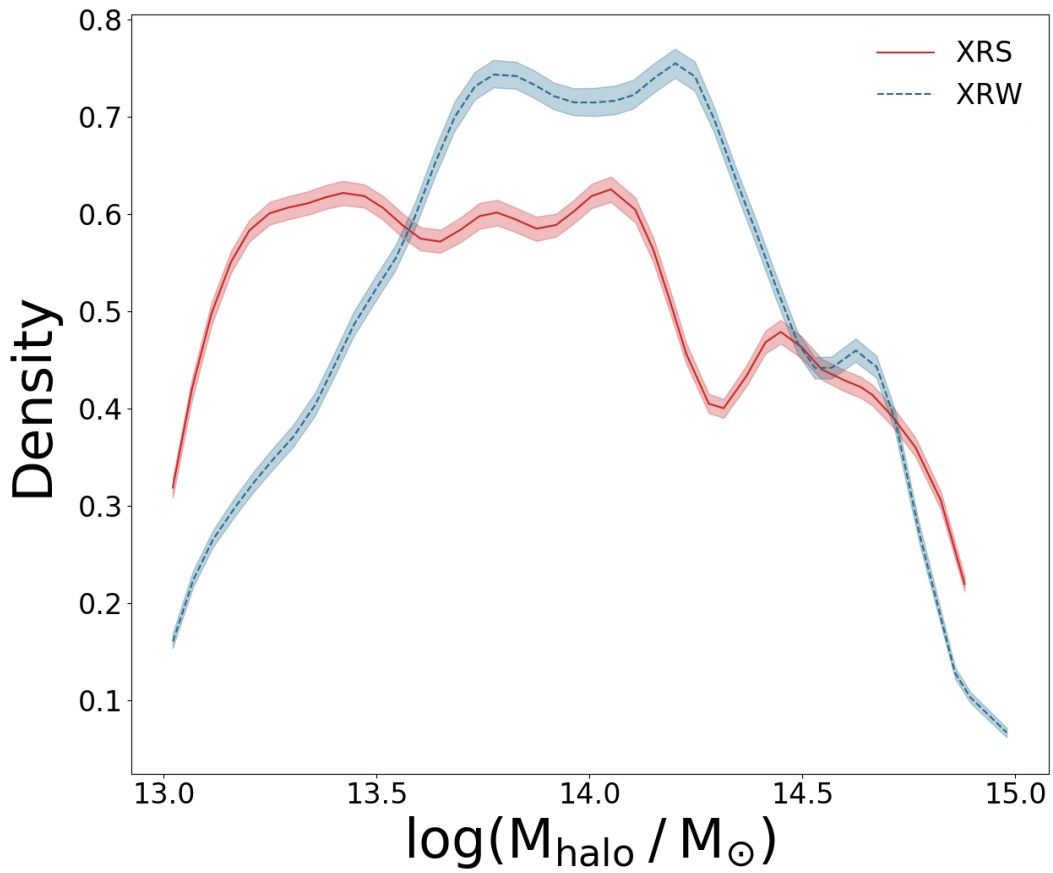


Figure 2.2 Smoothed density distributions of halo masses in the XRS (red) and XRW (blue) group samples. Shaded regions correspond to the 16th and 84th confidence levels from 1000 bootstrap resamplings.

2.2.3 Final Catalogues

2.2.3.1 Group samples

Our total final sample consists of 23,583 galaxies in 3,680 groups, and each galaxy has measured structural parameters from S11 and Mendel et al. (2014). Since our final samples are not volume-limited, we correct for the Malmquist bias by applying V_{max} weights (given by S11) to our results.

The group sample spans a redshift range of $0.01 \lesssim z \lesssim 0.1$, stellar mass range of $9 \lesssim \log(M_*/M_\odot) \lesssim 11.4$ and halo mass range of $13 \lesssim \log(M_{\text{halo}}/M_\odot) \lesssim 15$. To study the effects of the group environment¹ on galaxies, we divide our group sample into two approximately equal subsamples, based on whether a given group lies above or below the line of best fit in the $L_x - M_{\text{halo}}$ plane (see Wang et al., 2014; Roberts et al., 2016). The galaxies in groups above the line of best fit are hereafter referred to as the X-ray strong (XRS) sample, and the galaxies that are members of groups below the line of best fit are referred to as the X-ray weak (XRW) sample (see Fig. 2.1).

We also target the most extreme ends of our dataset in the $L_x - M_{\text{halo}}$ plane, by shifting the y-intercept of the line of best fit upwards (or downwards), until the top (or bottom) decile of the dataset is isolated. We will subsequently refer to these extreme ends of our sample as extremely X-ray strong (ex-XRS) and extremely X-ray weak (ex-XRW) (see §2.4.2).

¹ Typically clusters are defined to have halo masses of $\log(M_{\text{halo}}/M_\odot) \gtrsim 14$, but throughout our work we refer to all systems with $\log(M_{\text{halo}}/M_\odot) > 13$ as groups.

2.2.3.2 Isolated field sample

We compare our group sample to a field population of 38,657 galaxies with measured structural parameters, using an isolated field catalogue constructed by Roberts & Parker (2017) based on Y07. Roberts & Parker (2017) apply isolation criteria to single member group galaxies from Y07 such that: the projected group-centric distance of each galaxy is greater than 3 virial radii; each galaxy has a line-of-sight velocity greater than 1.5σ from the group centre, where σ is the velocity dispersion of the group centre (calculated from Eqn. 6 in Y07); and each galaxy is separated from its nearest bright neighbour by a minimum of 1 Mpc in projected distance and 1000 km s^{-1} in line-of-sight velocity. In this work, bright neighbours are defined as galaxies which are brighter than the SDSS survey r band magnitude limit at $z = 0.1$, $M_{r,lim} = -20.1$. Galaxies that are within 1 Mpc of SDSS survey edges are removed, as well as galaxies within 1000 km s^{-1} of $z = 0.1$ since we cannot be certain that such galaxies are not part of groups that extend beyond the boundaries of the survey area.

2.3 Results

2.3.1 Trends with Stellar Mass

To determine whether X-ray environment affects galaxy size and disc properties, we consider trends at fixed stellar mass, and later in narrow bins of group-centric radii and halo mass. We do not account for the increase of the fraction of star-forming galaxies in clusters with redshift (see the Butcher-Oemler effect Butcher & Oemler, 1984) since our sample is at $z < 0.1$.

2.3.1.1 Mass-size relation

We show the mass-size relation (effective radius versus stellar mass) for our three samples in Fig. 2.3. We see clear differences at low stellar masses, with isolated field galaxies having effective radii ~ 0.5 kpc larger than group galaxies (consistent with Tasca et al., 2009; Maltby et al., 2010; Fernández Lorenzo et al., 2013). There is also a systematic difference between our XRS and XRW samples at low stellar mass. At high stellar masses, the mass-size relation is independent of environment (in agreement with Pohlen & Trujillo, 2006; Maltby et al., 2010; Maltby et al., 2015). While the difference in the shape of the mass-size relation at low and high stellar masses remains to be fully explained, Fernández Lorenzo et al. (2013) examine the mass-size relation for galaxies of different morphological types and find that the flattening of the mass-size relation at low stellar masses is largely driven by late-type spirals. At higher stellar masses, the slope of the mass-size relation steepens and is dominated by early-type galaxies. Similarly, Cappellari (2016) shows that the mass-size relation below $\sim 10^{11} M_{\odot}$ is dominated by fast rotator early-type galaxies and late-type spirals, and slow rotator early-type galaxies drive the relation at higher stellar masses. Conversely, Mosleh et al. (2013) find that the shape of the mass-size relation is the same for both early and late-type galaxies, where the relation is flat below $\sim 10^{10} M_{\odot}$ and steepens at higher stellar masses. They suggest that for early-type compact galaxies at low stellar mass (less than $\sim 10^{9.5} M_{\odot}$), the flattening of the mass-size relation could be driven by fact that these galaxies have comparable sizes to the point-spread function (PSF). Since our sample at low stellar mass mainly consists of disc-dominated galaxies, our results are robust despite uncertainties associated with the PSF. We will explore the dependence of galaxy disc scale length on morphological type in §2.4.4.

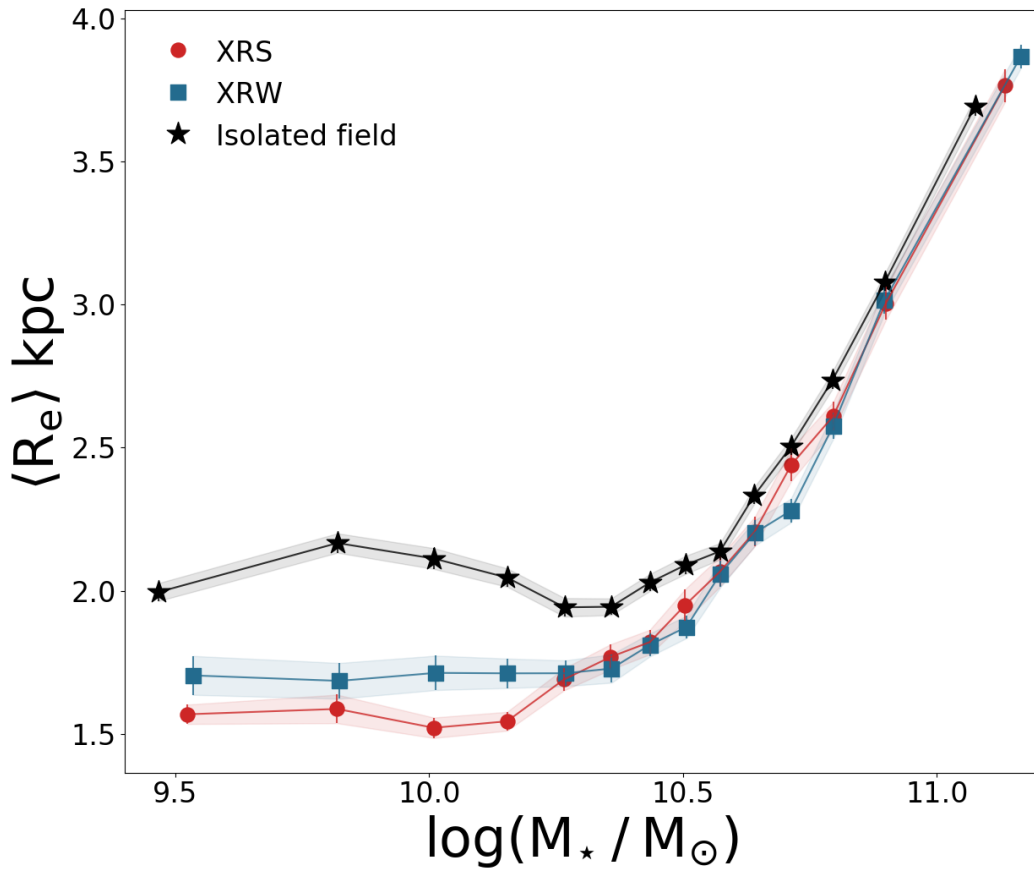


Figure 2.3 V_{max} weighted effective radius versus stellar mass for X-ray strong (XRS), X-ray weak (XRW), and isolated field samples. Error bars correspond to the standard error on the mean bin values, and are connected with shaded regions.

2.3.1.2 Disc properties at fixed stellar mass

As shown in Fig. 2.4, the exponential disc scale length increases with stellar mass (in agreement with Jaffé et al., 2018) in all of our samples. At stellar masses below $\sim 10^{10.5} M_{\odot}$ the group galaxies (XRS and XRW) have smaller discs than the isolated field galaxies. At higher stellar masses, the disc scale lengths of the group galaxies match those of the isolated field sample. We similarly find that the disc-to-total mass ratio ($D/T = M_{\text{disc}}/M_{\star, \text{total}}$) decreases with increasing stellar mass (Fig. 2.5). Galaxies with lower stellar masses in the isolated field have larger disc masses than in groups.

Fig. 2.4 and Fig. 2.5 show differences between galaxies in XRS and XRW group environments. We find that at low stellar mass stellar discs in XRS groups are slightly smaller than discs in XRW groups. It is worth noting that exploring disc properties at fixed galaxy stellar mass is not very sensitive to changes in the disc. Since we are specifically interested in the influence of environment on stellar discs, examining disc properties at fixed bulge mass allows us to directly study the effects of environment on discs separately, and prevents diluting the signal by studying discs at fixed total galaxy stellar mass.

2.3.2 Disc Properties at Fixed Bulge Mass

To more directly account for possible changes in the stellar disc with environment, we investigate how disc properties change with environment at fixed bulge mass rather than at fixed stellar mass (a similar approach has been used in recent works such as Lackner & Gunn, 2013; Bluck et al., 2014; Lang et al., 2014).

In Fig. 2.6, we observe that the disc scale length increases with bulge mass in the group (XRS and XRW) and isolated field samples. At low bulge masses, disc scale lengths are largest in the isolated field, smaller in XRW group envi-

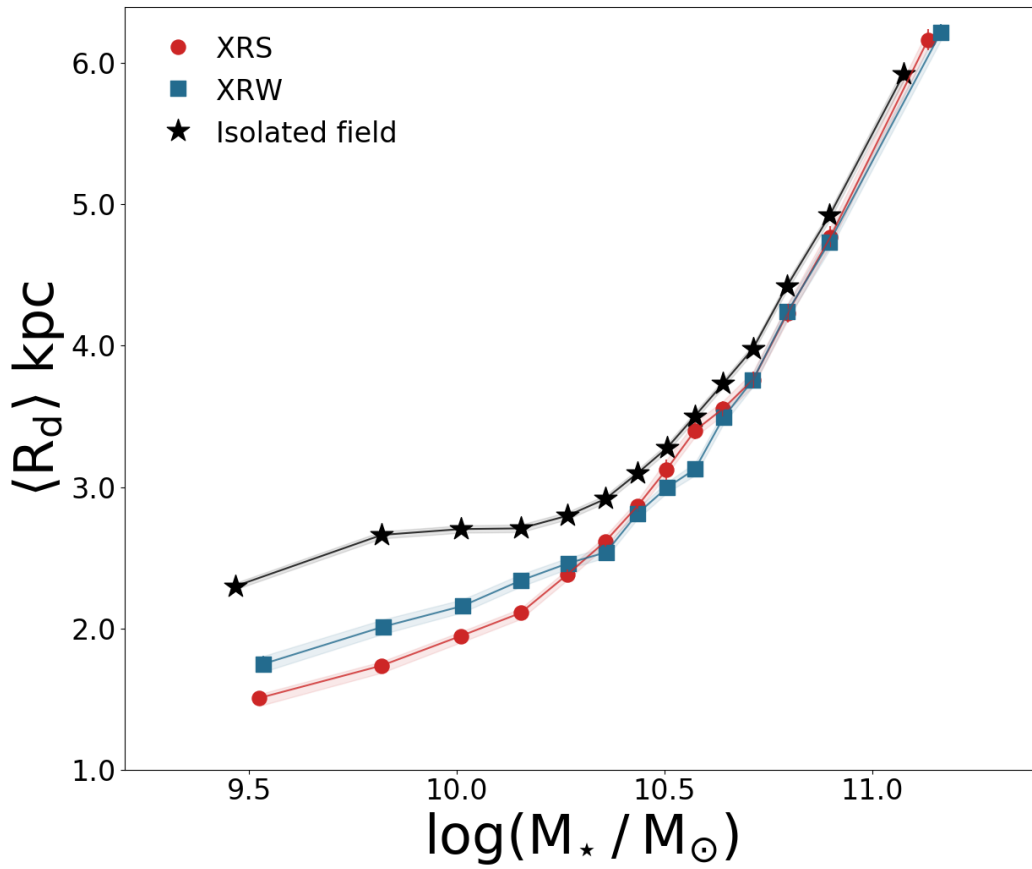


Figure 2.4 V_{max} weighted exponential disc scale length versus stellar mass. Error bars correspond to the standard error on the mean bin values, and are connected with shaded regions.

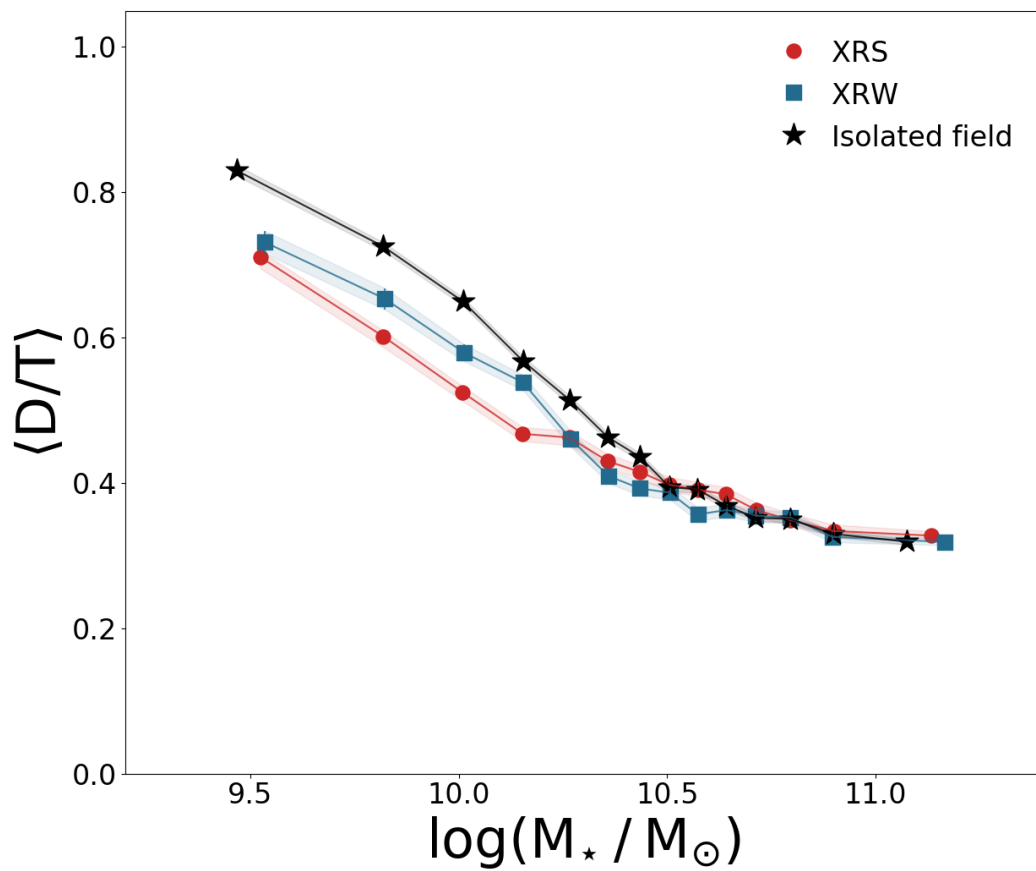


Figure 2.5 V_{max} weighted disc-to-total mass ratio versus stellar mass. Error bars correspond to the standard error on the mean bin values, and are connected with shaded regions.

ronments, and smallest in XRS environments. Qualitatively, these are the same trends we see at fixed stellar mass in Fig. 2.4, however the differences between samples are much larger at fixed bulge mass. The disc scale lengths of galaxies in the XRS sample are smaller than in the isolated field by ~ 1 kpc or $\sim 50\%$ at low bulge mass. We also find that the disc scale lengths of galaxies in XRS groups are systematically smaller than those of galaxies in XRW groups by ~ 0.5 kpc at low bulge mass. Similarly in Fig. 2.7, the disc-to-total mass ratio (D/T) decreases with increasing bulge mass. Moreover, at low bulge mass isolated field galaxies have the most massive discs and XRS group galaxies have the least massive discs.

2.3.3 Trends with Environmental Density

To further explore environmental dependencies, in Fig. 2.8 we show disc scale length versus bulge mass in bins of group-centric radius (normalized by R_{200m}) and halo mass. We note that the X-ray brightness of our XRS and XRW groups was previously defined at fixed halo mass in §2.2.3.1, and in this section we bin further by halo mass within our defined XRS and XRW samples. In Fig. 2.8, the faded lines correspond to the average trend for total XRS, XRW, and isolated field samples shown in Fig. 2.6. Overlaid on the average trends, in each panel we show the data in a given bin of group-centric distance and halo mass. Group-centric distance increases from top to bottom row, and halo mass increases from left to right. For example, the top left panel shows XRS and XRW data for small group-centric distances and low halo masses, overlaid on our average trends. Looking at all 9 panels, we find that the majority of our XRS and XRW samples in different halo masses and at varying group-centric distances are very similar to the average trends. Our findings are largely consistent with Lackner & Gunn (2013), who show that galaxy disc scale length at fixed bulge mass is independent of local density.

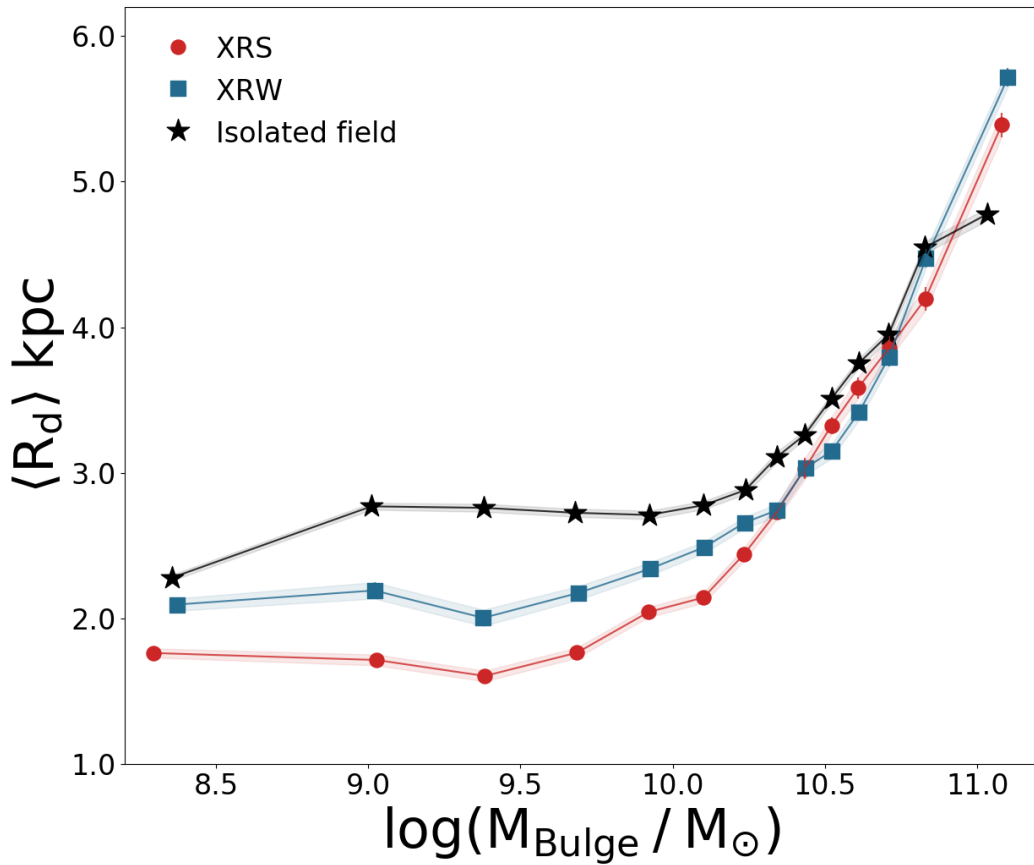


Figure 2.6 V_{max} weighted exponential disc scale length versus bulge mass. Error bars correspond to the standard error on the mean bin values, and are connected with shaded regions.

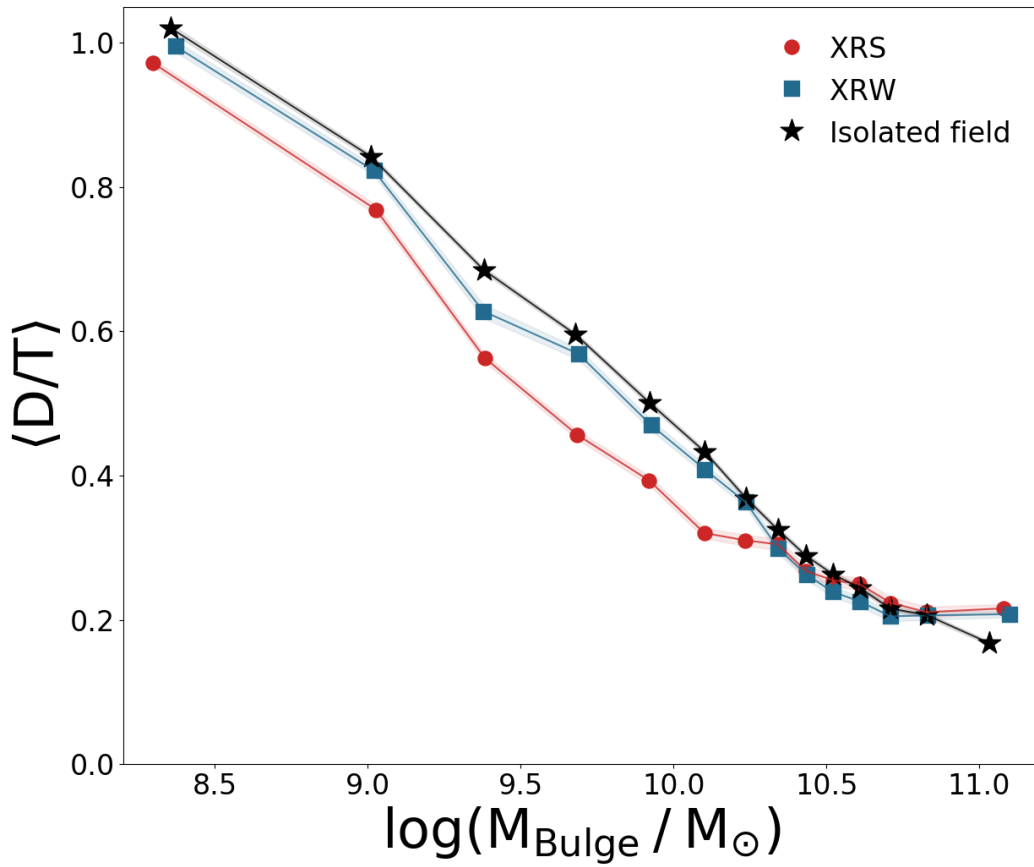


Figure 2.7 V_{max} weighted disc-to-total mass ratio versus bulge mass. Error bars correspond to the standard error on the mean bin values, and are connected with shaded regions.

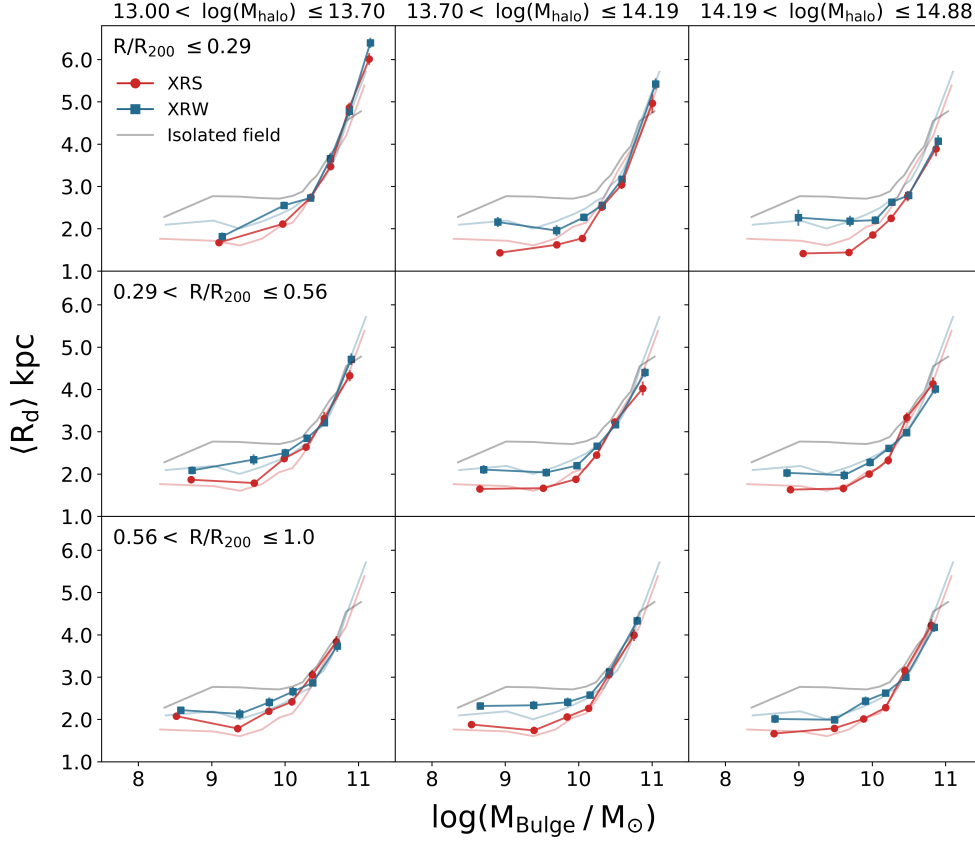


Figure 2.8 V_{max} weighted exponential disc scale length versus bulge mass, in bins of increasing group-centric radius (top to bottom) and increasing halo mass (left to right). Average trends from Fig. 2.6 correspond to the faded lines. Bold lines correspond to the trend in each environmental panel, where the error bars correspond to standard error of the mean.

However, there are two exceptions: at small group-centric radii and large halo masses (top right panel), the galaxies in our XRS sample have slightly smaller disc scale lengths than the average trend; on the opposite end, at large group-centric radii and low halo masses (bottom left panel), galaxies in the XRS sample have disc scale lengths that are above the average trend. These findings suggest that a combination of small group-centric distance and large halo mass leads to slightly enhance disc truncation in X-ray bright groups.

2.4 Discussion

2.4.1 Challenges with Galaxy Size Measurements

Reliable galaxy size measurements are notoriously challenging to obtain due to a variety of systematic effects. Mosleh et al. (2013) show that using a single component Sérsic model (as opposed to a two component or non-parametric model) yields systematic overestimates of galaxy sizes at local redshifts, possibly due to substructure being missed. Furthermore, for early-type galaxies that are compact, the point-spread function (PSF) becomes a significant fraction of galaxy sizes with $R_e < 1$ kpc. In late-type galaxies, the edges of discs that have low-surface brightness components are also difficult to detect, due to low signal-to-noise. Similarly, Simard et al. (2002) state that bulge + disc structural parameters are most affected by systematic errors from sky background level determinations. If the sky level is underestimated, disc component sizes are overestimated due to positive sky residuals. Additionally, crowding errors and fibre errors in the SDSS reddened galaxy colours, and these errors affect size determinations from surface brightness profile fits (see S11 for their treatment of these errors). To distinguish the validity of applying bulge-disc decompositions, versus pure Sérsic models to SDSS galaxies, S11 provide a parameter P_{pS} constructed using the F-statistic. P_{pS} is defined as the probability that a bulge + disc model is not required compared to a single component Sérsic model. To distinguish which galaxies are best represented by genuine bulge + disc systems, it is recommended to use a $P_{pS} \leq 0.32$ cut. We applied the $P_{pS} \leq 0.32$ to our work, and the relative differences between isolated field, XRW and XRS samples remain unchanged.

The presence of dust in discs (e.g. Driver et al., 2007) can also change the intrinsic disc size-luminosity and colour-luminosity relations - although there is no simple prescription for applying empirical dust corrections to separate

structural components of galaxies. Selecting face-on discs can mitigate the effects of dust; however, since our galaxies in XRS, XRW and isolated field samples have similar distributions in inclination, we did not apply dust corrections to our data. Overall, despite the challenges with determining individual galaxy sizes, we emphasize that this work is a relative comparison between three large samples with similar systematics. The relative differences between disc properties at fixed bulge mass in our samples are robust despite these uncertainties.

2.4.2 X-Ray Extreme Environments

Our results in Fig. 2.6 show that galaxy disc scale length depends on group X-ray brightness. However, since the scatter in the X-ray luminosity for a given group is large (of order 0.4 dex in Wang et al., 2014), we also look at our trends in disc scale length at fixed bulge mass for the extreme ends of the $L_x - M_{halo}$ plane (samples are labelled ex-XRS and ex-XRW in Fig. 2.1) to ensure that the trends we observe with X-ray brightness are robust. In Fig. 2.9 we see that compared to our average trends, galaxies in extremely X-ray bright environments are further truncated, and in extremely X-ray faint environments galaxy disc scale lengths approach the trends for the isolated field sample. The enhancement of disc truncation in extremely X-ray strong systems confirms that the differences we see are not simply a result of scatter in the $L_x - M_{halo}$ relation, since the trends exhibit a stronger dependence on X-ray luminosity in the extremes of the dataset.

2.4.3 Star-forming and Quiescent Discs

At higher redshifts ($z \sim 0.44$), Kuchner et al. (2017) find that late-type galaxies in cluster environments have smaller disc sizes than in the field. At

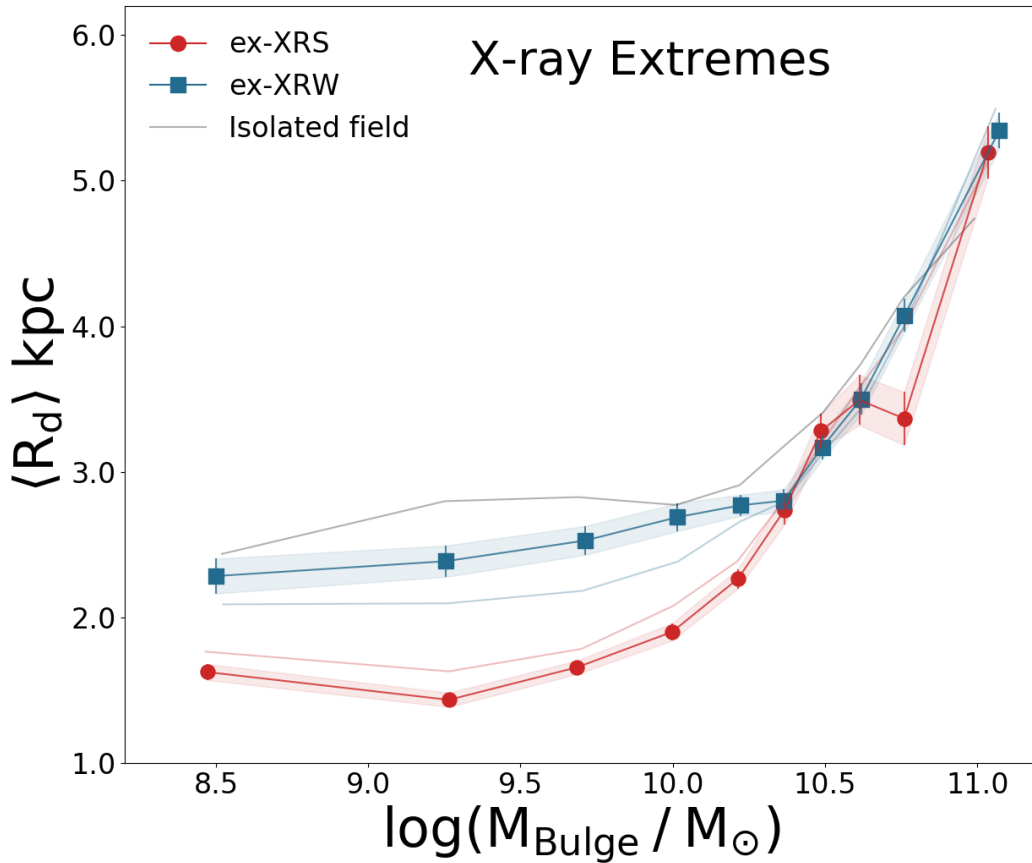


Figure 2.9 V_{max} weighted exponential disc scale length versus bulge mass. Bold lines correspond to galaxies in extremely XRS and extremely XRW environments. Faded lines correspond to average trends for entire sample in Fig. 2.6. Error bars correspond to the standard error on the mean bin values, and are connected with shaded regions.

fixed bulge-to-total mass ratio ($B/T = M_{\text{bulge}}/M_{\star}$) and stellar mass, they show that quiescent spirals are smaller than star-forming spirals. After comparing disc sizes of quiescent and star-forming galaxies, they find that the outer disc “fades” in quiescent discs. They attribute these results to a combination of ram-pressure stripping and other slow gas removal processes such as starvation. However, previous work (e.g. Shioya et al., 2002) shows that truncated spirals only become red and quenched ~ 1 Gyr after disc truncation using chemical evolution models.

To explore whether the galaxies in our samples undergo disc-fading from the outside-in, we make a simple cut in specific star-formation rate ($\text{SSFR} = \text{SFR}/M_{\star}$) using star-formation rates (SFR) from Brinchmann et al. (2004) and stellar masses from Mendel et al. (2014). The “break” between the red quiescent and blue star-forming population of galaxies at low-redshift occurs at $\log \text{SSFR} \sim -11 \text{ yr}^{-1}$ (Wetzell et al., 2012). In Fig. 2.10 we show our results for galaxies classified as star-forming (with $\log \text{SSFR} > -11 \text{ yr}^{-1}$) overlaid on the average trends for the full sample (see Fig. 2.6). For $\log(M_{\text{bulge}}/M_{\odot}) \lesssim 10.5$, star-forming galaxies in XRS and XRW environments have a steeper dependence on bulge mass and have significantly larger disc-scale lengths than the average trends from the total sample. The fact that star-forming discs are larger than our average trends suggests that as a star-forming disc quenches, its exponential disc scale length decreases from the outside-in. These findings could be an indication that we are observing outside-in disc fading occurring in our sample.

2.4.4 Trends by Morphological Type

To determine whether our trends are specific to early or late-type morphological classifications within our sample, we use the machine learning catalogue of Huertas-Company et al. (2011) that divides SDSS galaxies into four types:

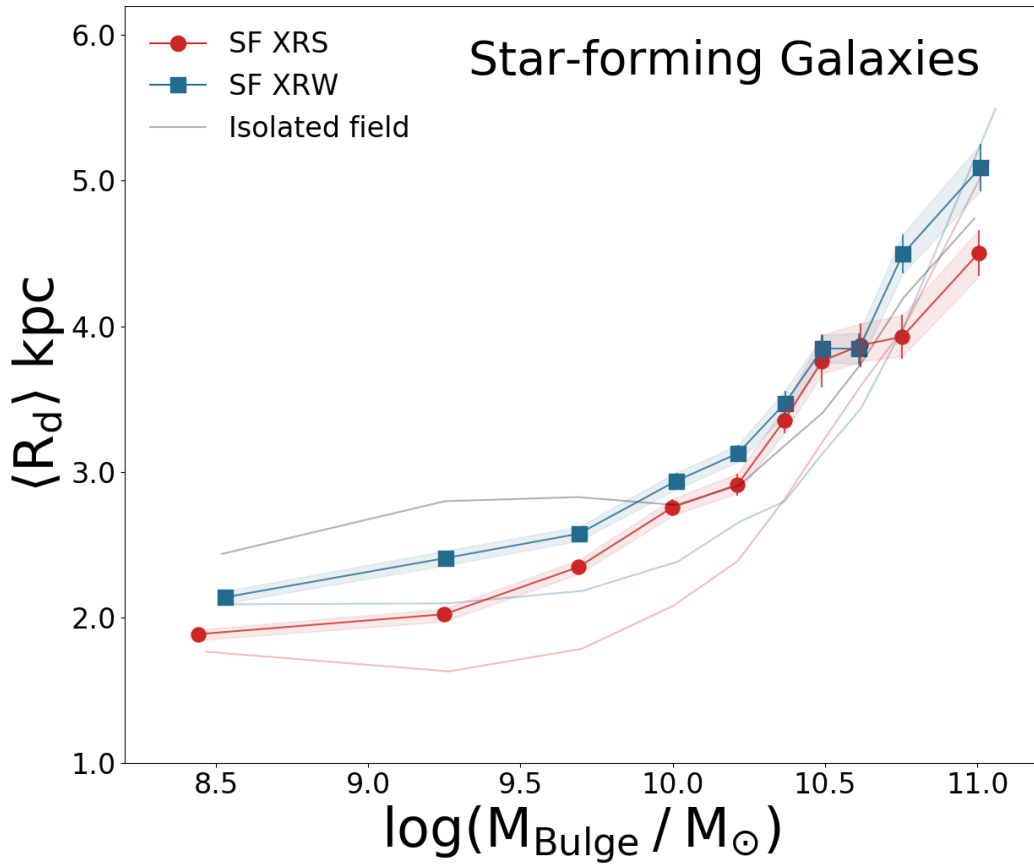


Figure 2.10 V_{max} weighted exponential disc scale length versus bulge mass. Bold lines correspond to star-forming galaxies. Faded lines correspond to average trends for entire sample in Fig. 2.6. Error bars correspond to the standard error on the mean bin values, and are connected with shaded regions.

ellipticals (E), lenticular galaxies (S0), intermediate spirals (Sa/Sb) and late-type spirals (Sc/Sd). Since there are biases in detecting differences between E/S0 galaxies in the Huertas-Company et al. (2011) catalogue and we are primarily interested in discs, we remove these early-types from our analysis. In Fig. 2.11, we see that Sc/Sds have significantly larger disc scale lengths compared to Sa/Sbs, consistent with previous work (e.g. Courteau et al., 2007; Vaghmare et al., 2015). When we subdivide these morphological types by isolated field, XRS and XRW environments, we find that the disc scale lengths of spiral galaxies (Sa/Sb and Sc/Sd) at fixed bulge mass exhibit the same trends with environment as Fig. 2.6: that is, isolated field $>$ XRW $>$ XRS. We see a clear separation of disc sizes with X-ray environment for both types of spiral morphologies.

2.4.5 Putting it all Together

We find that galaxy disc properties are sensitive to X-ray environment, a tracer of IGM density. At fixed stellar mass, Fig. 2.4 and Fig. 2.5 show that galaxies in group environments have smaller disc scale lengths and disc-to-total mass ratios than isolated field galaxies. However, by fixing stellar mass our results are much less sensitive to changes in galaxy discs with environment. Examining discs at fixed bulge mass is a more direct way to explore disc properties. In Fig. 2.6 we see that galaxy stellar discs in XRS group environments are strongly truncated as compared to discs in XRW groups and isolated field environments. There are a number of processes that could lead to discs being truncated in groups compared to the field, but the fact that discs are more truncated in XRS groups compared to XRW groups suggests that IGM density plays an important role. Since hydrodynamical processes are most effective in the densest IGMs, we expect environmental mechanisms such as starvation and ram-pressure stripping to be most efficient in XRS group

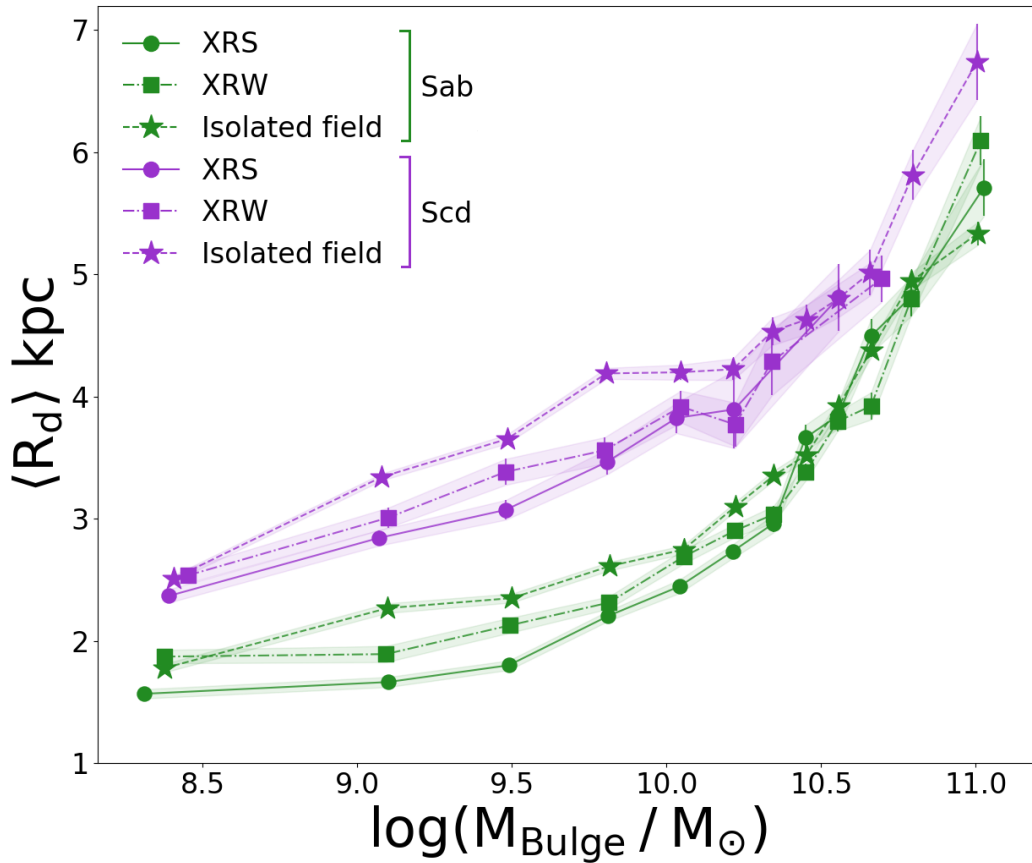


Figure 2.11 V_{max} weighted exponential disc scale length versus bulge mass by morphological type (Sa/Sbs in green and Sc/Sds in purple). Dashed lines are isolated field galaxies, XRW are dot-dashed and XRS are solid. Error bars correspond to the standard error on the mean bin values, and are connected with shaded regions.

environments. The fact that the differences in disc properties are enhanced in the X-ray extremes of our dataset is consistent with a hydrodynamic origin.

Additionally, in Fig. 2.8 we find that disc scale length does not depend on group-centric radius or halo mass, except for a mild enhancement in disc truncation close to the centres of cluster-sized halos. The fact that galaxies in XRS environments are truncated regardless of halo mass and group-centric position could be interpreted as evidence for a process such as starvation, since our results suggest that the main influence on disc morphology is whether or not a galaxy inhabits a dense IGM (Larson et al., 1980; Bekki et al., 2002; van den Bosch et al., 2008; Schawinski et al., 2014). However, there is evidence of gas accretion rates onto galaxies decreasing towards smaller group-centric radii (van de Voort et al., 2017), which leads to suppression of SFR near group-centres compared to group outskirts (Wetzel et al., 2012; Paccagnella et al., 2016). In turn, the suppression of SFRs near group-centres could cause stellar disc sizes to follow group-centric radial trends as well. The fact that we do not see these radial trends with disc scale length could be due to morphological quenching stabilizing the stellar disc (e.g. Dekel & Birnboim, 2008; Martig et al., 2009, 2013). Morphology scaling relations at fixed stellar mass have long been shown to only weakly depend on environmental density (e.g. Bamford et al., 2009), in agreement with our findings. Although, in Fig. 2.8 we also see a mild enhancement of disc truncation at small group-centric radii in large halos, and we suggest that the enhancement we see could be due to the added effect of ram-pressure stripping; since these galaxies would be moving fastest, and through the densest IGMs. Detailed exploration of the possible physical mechanisms at play awaits future work. What is clear is that disc properties are sensitive to X-ray brightness.

2.5 Conclusions

We study a sample galaxies from SDSS-DR7 in the Y07 group catalogue with X-ray data from Wang et al. (2014) and bulge-disc structural parameters from S11 and Mendel et al. (2014). We find that:

1. The exponential disc scale lengths of low mass galaxies in groups (both X-ray strong and X-ray weak) are smaller than isolated field galaxies by ~ 1 kpc, consistent with previous work. Additionally, the discs of low mass galaxies in XRS groups are truncated by ~ 0.5 kpc compared to galaxies in XRW groups.
2. Disc scale length at fixed bulge mass in our XRS, XRW and isolated field samples is largely independent of group-centric distance and halo mass, with the exception of a slight enhancement of disc truncation at small group-centric radii and large halo masses.
3. Disc truncation is enhanced in the most extreme X-ray strong (ex-XRS) systems.
4. Star-forming spiral galaxies in XRS and XRW environments have larger stellar discs than the average trends for our total group samples.
5. Sa/Sb spiral galaxies have smaller disc scale lengths than Sc/Sd galaxies. Both Sa/Sb and Sc/Sd subsets of spiral galaxies are largest in the isolated field sample, intermediate in XRW groups, and most truncated in XRS groups.

Together these findings clearly demonstrate the impact of X-ray environment on galaxy disc properties for low mass galaxies. Future studies with resolved Integrated Field Unit (IFU) maps could be used to extract star-forming radii to compare to the disc scale lengths from traditional bulge-disc decompositions. Taken one step further, applying bulge-disc decompositions to IFU

datacubes directly (Johnston et al., 2017) and analyzing how galaxy structural components vary with environment could shed light on the transformation of galaxy disc morphology.

Bibliography

Abadi, M. G., Moore, B., & Bower, R. G. 1999, *MNRAS*, 308, 947

Abazajian, K. N., Adelman-McCarthy, J. K., Agüeros, M. A., Allam, S. S., Prieto, C. A., An, D., Anderson, K. S. J., Anderson, S. F., Annis, J., Bahcall, N. A., Bailer-Jones, C. A. L., Barentine, J. C., Bassett, B. A., Becker, A. C., Beers, T. C., Bell, E. F., Belokurov, V., Berlind, A. A., Berman, E. F., Bernardi, M., Bickerton, S. J., Bizyaev, D., Blakeslee, J. P., Blanton, M. R., Bochanski, J. J., Boroski, W. N., Brewington, H. J., Brinchmann, J., Brinkmann, J., Brunner, R. J., Budavári, T., Carey, L. N., Carliles, S., Carr, M. A., Castander, F. J., Cinabro, D., Connolly, A. J., Csabai, I., Cunha, C. E., Czarapata, P. C., Davenport, J. R. A., de Haas, E., Dilday, B., Doi, M., Eisenstein, D. J., Evans, M. L., Evans, N. W., Fan, X., Friedman, S. D., Friedman, J. A., Fukugita, M., Gänsicke, B. T., Gates, E., Gillespie, B., Gilmore, G., Gonzalez, B., Gonzalez, C. F., Grebel, E. K., Gunn, J. E., Györy, Z., Hall, P. B., Harding, P., Harris, F. H., Harvanek, M., Hawley, S. L., Hayes, J. J. E., Heckman, T. M., Hendry, J. S., Hennessy, G. S., Hindsley, R. B., Hoblitt, J., Hogan, C. J., Hogg, D. W., Holtzman, J. A., Hyde, J. B., Ichi Ichikawa, S., Ichikawa, T., Im, M., Ivezić, Ž., Jester, S., Jiang, L., Johnson, J. A., Jorgensen, A. M., Jurić, M., Kent, S. M., Kessler, R., Kleinman, S. J., Knapp, G. R., Konishi, K., Kron, R. G., Krzesinski, J., Kuropatkin, N., Lampeitl, H., Lebedeva, S., Lee, M. G., Lee, Y. S., Leger, R. F., Lépine, S., Li, N., Lima, M., Lin, H., Long, D. C., Loomis, C. P., Loveday, J., Lupton, R. H., Magnier, E., Malanushenko, O., Malanushenko, V., Mandelbaum, R., Margon, B., Marriner, J. P., Martínez-Delgado, D., Matsubara, T., McGehee, P. M., McKay, T. A., Meiksin, A., Morrison, H. L., Mullally, F., Munn, J. A., Murphy, T., Nash, T., Nebot, A., Neilsen, E. H., Newberg, H. J.,

- Newman, P. R., Nichol, R. C., Nicinski, T., Nieto-Santisteban, M., Nitta, A., Okamura, S., Oravetz, D. J., Ostriker, J. P., Owen, R., Padmanabhan, N., Pan, K., Park, C., Pauls, G., Peoples, J., Percival, W. J., Pier, J. R., Pope, A. C., Pourbaix, D., Price, P. A., Purger, N., Quinn, T., Raddick, M. J., Fiorentin, P. R., Richards, G. T., Richmond, M. W., Riess, A. G., Rix, H.-W., Rockosi, C. M., Sako, M., Schlegel, D. J., Schneider, D. P., Scholz, R.-D., Schreiber, M. R., Schwobe, A. D., Seljak, U., Sesar, B., Sheldon, E., Shimasaku, K., Sibley, V. C., Simmons, A. E., Sivarani, T., Smith, J. A., Smith, M. C., Smolčić, V., Snedden, S. A., Stebbins, A., Steinmetz, M., Stoughton, C., Strauss, M. A., SubbaRao, M., Suto, Y., Szalay, A. S., Szapudi, I., Szkody, P., Tanaka, M., Tegmark, M., Teodoro, L. F. A., Thakar, A. R., Tremonti, C. A., Tucker, D. L., Uomoto, A., Berk, D. E. V., Vandenberg, J., Vidrih, S., Vogeley, M. S., Voges, W., Vogt, N. P., Wadadekar, Y., Watters, S., Weinberg, D. H., West, A. A., White, S. D. M., Willhite, B. C., Wonders, A. C., Yanny, B., Yocum, D. R., York, D. G., Zehavi, I., Zibetti, S., & Zucker, D. B. 2009, *ApJS*, 182, 543
- Andredakis, Y. C., Peletier, R. F., & Balcells, M. 1995, *MNRAS*, 275, 874
- Angulo, R. E., Lacey, C. G., Baugh, C. M., & Frenk, C. S. 2009, *MNRAS*, 399, 983
- Baldry, I. K., Balogh, M. L., Bower, R. G., Glazebrook, K., Nichol, R. C., Bamford, S. P., & Budavari, T. 2006, *MNRAS*, 373, 469
- Balogh, M. L., Baldry, I. K., Nichol, R., Miller, C., Bower, R., & Glazebrook, K. 2004, *ApJ*, 615, L101
- Bamford, S. P., Nichol, R. C., Baldry, I. K., Land, K., Lintott, C. J., Schawinski, K., Slosar, A., Szalay, A. S., Thomas, D., Tori, M., Andreescu, D., Edmondson, E. M., Miller, C. J., Murray, P., Raddick, M. J., & Vandenberg, J. 2009, *MNRAS*, 393, 1324

- Bekki, K., Couch, W. J., & Shioya, Y. 2002, *ApJ*, 577, 651
- Bluck, A. F. L., Mendel, J. T., Ellison, S. L., Moreno, J., Simard, L., Patton, D. R., & Starkenburg, E. 2014, *MNRAS*, 441, 599
- Bösch, B., Böhm, A., Wolf, C., Aragón-Salamanca, A., Barden, M., Gray, M. E., Ziegler, B. L., Schindler, S., & Balogh, M. 2013, *A&A*, 549, A142
- Boselli, A., Boissier, S., Cortese, L., Gil de Paz, A., Seibert, M., Madore, B. F., Buat, V., & Martin, D. C. 2006, *ApJ*, 651, 811
- Brinchmann, J., Charlot, S., White, S. D. M., Tremonti, C., Kauffmann, G., Heckman, T., & Brinkmann, J. 2004, *MNRAS*, 351, 1151
- Butcher, H. & Oemler, Jr., A. 1984, *ApJ*, 285, 426
- Calzetti, D., Armus, L., Bohlin, R. C., Kinney, A. L., Koornneef, J., & Storchi-Bergmann, T. 2000, *ApJ*, 533, 682
- Capaccioli, M. 1989, in *World of Galaxies (Le Monde des Galaxies)*, ed. H. G. Corwin, Jr. & L. Bottinelli, 208–227
- Cappellari, M. 2016, *ARA&A*, 54, 597
- Cimatti, A., Cassata, P., Pozzetti, L., Kurk, J., Mignoli, M., Renzini, A., Daddi, E., Bolzonella, M., Brusa, M., Rodighiero, G., Dickinson, M., Franceschini, A., Zamorani, G., Berta, S., Rosati, P., & Halliday, C. 2008, *A&A*, 482, 21
- Cohn, J. D. 2012, *MNRAS*, 419, 1017
- Conroy, C. & Gunn, J. E. 2010, *ApJ*, 712, 833
- Conroy, C., Gunn, J. E., & White, M. 2009, *ApJ*, 699, 486
- Conroy, C., White, M., & Gunn, J. E. 2010, *ApJ*, 708, 58

- Conselice, C. J., Yang, C., & Bluck, A. F. L. 2009, MNRAS, 394, 1956
- Cortese, L., Gavazzi, G., Boselli, A., Franzetti, P., Kennicutt, R. C., O’Neil, K., & Sakai, S. 2006, A&A, 453, 847
- Courteau, S., Dutton, A. A., van den Bosch, F. C., MacArthur, L. A., Dekel, A., McIntosh, D. H., & Dale, D. A. 2007, ApJ, 671, 203
- Daddi, E., Renzini, A., Pirzkal, N., Cimatti, A., Malhotra, S., Stiavelli, M., Xu, C., Pasquali, A., Rhoads, J. E., Brusa, M., di Serego Alighieri, S., Ferguson, H. C., Koekemoer, A. M., Moustakas, L. A., Panagia, N., & Windhorst, R. A. 2005, ApJ, 626, 680
- Davis, M., Efstathiou, G., Frenk, C. S., & White, S. D. M. 1985, ApJ, 292, 371
- de Jong, R. S. 1996, A&A, 313, 45
- Dekel, A. & Birnboim, Y. 2008, MNRAS, 383, 119
- Dressler, A. 1980, ApJ, 236, 351
- Driver, S. P., Allen, P. D., Graham, A. W., Cameron, E., Liske, J., Ellis, S. C., Cross, N. J. G., De Propriis, R., Phillipps, S., & Couch, W. J. 2006, MNRAS, 368, 414
- Driver, S. P., Popescu, C. C., Tuffs, R. J., Liske, J., Graham, A. W., Allen, P. D., & de Propriis, R. 2007, MNRAS, 379, 1022
- Dutton, A. A., van den Bosch, F. C., Faber, S. M., Simard, L., Kassin, S. A., Koo, D. C., Bundy, K., Huang, J., Weiner, B. J., Cooper, M. C., Newman, J. A., Mozena, M., & Koekemoer, A. M. 2011, MNRAS, 410, 1660
- Evans, F. A., Parker, L. C., & Roberts, I. D. 2018, MNRAS, 476, 5284

Fernández Lorenzo, M., Sulentic, J., Verdes-Montenegro, L., & Argudo-Fernández, M. 2013, MNRAS, 434, 325

Fujita, Y. 2004, PASJ, 56, 29

Fujita, Y. & Nagashima, M. 1999, ApJ, 516, 619

Gómez, P. L., Nichol, R. C., Miller, C. J., Balogh, M. L., Goto, T., Zabludoff, A. I., Romer, A. K., Bernardi, M., Sheth, R., Hopkins, A. M., Castander, F. J., Connolly, A. J., Schneider, D. P., Brinkmann, J., Lamb, D. Q., SubbaRao, M., & York, D. G. 2003, ApJ, 584, 210

Goto, T., Yamauchi, C., Fujita, Y., Okamura, S., Sekiguchi, M., Smail, I., Bernardi, M., & Gomez, P. L. 2003, MNRAS, 346, 601

Graham, A. W. 2012, ApJ, 746, 113

Graham, A. W. 2014, in Astronomical Society of the Pacific Conference Series, Vol. 480, Structure and Dynamics of Disk Galaxies, ed. M. S. Seigar & P. Treuhardt, 185

Gunn, J. E. & Gott, III, J. R. 1972, ApJ, 176, 1

Häring, N. & Rix, H.-W. 2004, ApJ, 604, L89

Hogg, D. W. 1999, ArXiv Astrophysics e-prints

Huchra, J. P. & Geller, M. J. 1982, ApJ, 257, 423

Hudson, M. J., Stevenson, J. B., Smith, R. J., Wegner, G. A., Lucey, J. R., & Simard, L. 2010, MNRAS, 409, 405

Huertas-Company, M., Aguerri, J. A. L., Bernardi, M., Mei, S., & Sánchez Almeida, J. 2011, A&A, 525, A157

Jaffé, Y. L., Poggianti, B. M., Moretti, A., Gullieuszik, M., Smith, R., Vulcani, B., Fasano, G., Fritz, J., Tonnesen, S., Bettoni, D., Hau, G., Biviano, A., Bellhouse, C., & McGee, S. 2018, *MNRAS*, 476, 4753

Johnston, E. J., Häußler, B., Aragón-Salamanca, A., Merrifield, M. R., Bamford, S., Bershad, M. A., Bundy, K., Drory, N., Fu, H., Law, D., Nitschelm, C., Thomas, D., Roman Lopes, A., Wake, D., & Yan, R. 2017, *MNRAS*, 465, 2317

Joshi, G. D., Parker, L. C., & Wadsley, J. 2017, PhD thesis, McMaster University

Kapferer, W., Sluka, C., Schindler, S., Ferrari, C., & Ziegler, B. 2009, *A&A*, 499, 87

Kawata, D. & Mulchaey, J. S. 2008, *ApJ*, 672, L103

Kennicutt, Jr., R. C. 1989, *ApJ*, 344, 685

Kuchner, U., Ziegler, B., Verdugo, M., Bamford, S., & Häußler, B. 2017, *A&A*, 604, A54

Lackner, C. N. & Gunn, J. E. 2013, *MNRAS*, 428, 2141

Lang, P., Wuyts, S., Somerville, R. S., Förster Schreiber, N. M., Genzel, R., Bell, E. F., Brammer, G., Dekel, A., Faber, S. M., Ferguson, H. C., Groggin, N. A., Kocevski, D. D., Koekemoer, A. M., Lutz, D., McGrath, E. J., Momcheva, I., Nelson, E. J., Primack, J. R., Rosario, D. J., Skelton, R. E., Tacconi, L. J., van Dokkum, P. G., & Whitaker, K. E. 2014, *ApJ*, 788, 11

Larson, R. B., Tinsley, B. M., & Caldwell, C. N. 1980, *ApJ*, 237, 692

- Lewis, I., Balogh, M., De Propriis, R., Couch, W., Bower, R., Offer, A., Bland-Hawthorn, J., Baldry, I. K., Baugh, C., Bridges, T., Cannon, R., Cole, S., Colless, M., Collins, C., Cross, N., Dalton, G., Driver, S. P., Efstathiou, G., Ellis, R. S., Frenk, C. S., Glazebrook, K., Hawkins, E., Jackson, C., Lahav, O., Lumsden, S., Maddox, S., Madgwick, D., Norberg, P., Peacock, J. A., Percival, W., Peterson, B. A., Sutherland, W., & Taylor, K. 2002, *MNRAS*, 334, 673
- Longhetti, M., Saracco, P., Severgnini, P., Della Ceca, R., Mannucci, F., Bender, R., Drory, N., Feulner, G., & Hopp, U. 2007, *MNRAS*, 374, 614
- Magorrian, J., Tremaine, S., Richstone, D., Bender, R., Bower, G., Dressler, A., Faber, S. M., Gebhardt, K., Green, R., Grillmair, C., Kormendy, J., & Lauer, T. 1998, *AJ*, 115, 2285
- Makino, J. & Hut, P. 1997, *ApJ*, 481, 83
- Maltby, D. T., Aragón-Salamanca, A., Gray, M. E., Barden, M., Häußler, B., Wolf, C., Peng, C. Y., Jahnke, K., McIntosh, D. H., Böhm, A., & van Kampen, E. 2010, *MNRAS*, 402, 282
- Maltby, D. T., Aragón-Salamanca, A., Gray, M. E., Hoyos, C., Wolf, C., Jogee, S., & Böhm, A. 2015, *Monthly Notices of the Royal Astronomical Society*, 447, 1506
- Marconi, A. & Hunt, L. K. 2003, *ApJ*, 589, L21
- Martig, M., Bournaud, F., Teyssier, R., & Dekel, A. 2009, *ApJ*, 707, 250
- Martig, M., Crocker, A. F., Bournaud, F., Emsellem, E., Gabor, J. M., Alatalo, K., Blitz, L., Bois, M., Bureau, M., Cappellari, M., Davies, R. L., Davis, T. A., Dekel, A., de Zeeuw, P. T., Duc, P.-A., Falcón-Barroso, J., Khochfar, S., Krajnović, D., Kuntschner, H., Morganti, R., McDermid, R. M., Naab,

- T., Oosterloo, T., Sarzi, M., Scott, N., Serra, P., Griffin, K. S., Teyssier, R., Weijmans, A.-M., & Young, L. M. 2013, MNRAS, 432, 1914
- Masters, K. L., Mosleh, M., Romer, A. K., Nichol, R. C., Bamford, S. P., Schawinski, K., Lintott, C. J., Andreescu, D., Campbell, H. C., Crowcroft, B., Doyle, I., Edmondson, E. M., Murray, P., Raddick, M. J., Slosar, A., Szalay, A. S., & Vandenberg, J. 2010, MNRAS, 405, 783
- Mendel, J. T., Simard, L., Palmer, M., Ellison, S. L., & Patton, D. R. 2014, ApJS, 210, 3
- Moore, B., Katz, N., Lake, G., Dressler, A., & Oemler, A. 1996, Nature, 379, 613
- Moore, B., Lake, G., & Katz, N. 1998, ApJ, 495, 139
- Moran, S. M., Ellis, R. S., Treu, T., Salim, S., Rich, R. M., Smith, G. P., & Kneib, J.-P. 2006, ApJ, 641, L97
- Moran, S. M., Ellis, R. S., Treu, T., Smith, G. P., Rich, R. M., & Smail, I. 2007, ApJ, 671, 1503
- Mosleh, M., Williams, R. J., & Franx, M. 2013, ApJ, 777, 117
- Oemler, Jr., A. 1974, ApJ, 194, 1
- Okamoto, T. & Nagashima, M. 2003, ApJ, 587, 500
- Paccagnella, A., Vulcani, B., Poggianti, B. M., Moretti, A., Fritz, J., Gullieuszik, M., Couch, W., Bettoni, D., Cava, A., D'Onofrio, M., & Fasano, G. 2016, ApJ, 816, L25
- Peng, Y.-j., Lilly, S. J., Kovač, K., Bolzonella, M., Pozzetti, L., Renzini, A., Zamorani, G., Ilbert, O., Knobel, C., Iovino, A., Maier, C., Cucciati, O., Tasca, L., Carollo, C. M., Silverman, J., Kampczyk, P., de Ravel, L.,

- Sanders, D., Scoville, N., Contini, T., Mainieri, V., Scodreggio, M., Kneib, J.-P., Le Fèvre, O., Bardelli, S., Bongiorno, A., Caputi, K., Coppa, G., de la Torre, S., Franzetti, P., Garilli, B., Lamareille, F., Le Borgne, J.-F., Le Brun, V., Mignoli, M., Perez Montero, E., Pello, R., Ricciardelli, E., Tanaka, M., Tresse, L., Vergani, D., Welikala, N., Zucca, E., Oesch, P., Abbas, U., Barnes, L., Bordoloi, R., Bottini, D., Cappi, A., Cassata, P., Cimatti, A., Fumana, M., Hasinger, G., Koekemoer, A., Leauthaud, A., Maccagni, D., Marinoni, C., McCracken, H., Memeo, P., Meneux, B., Nair, P., Porciani, C., Presotto, V., & Scaramella, R. 2010, *ApJ*, 721, 193
- Poggianti, B. M., Fasano, G., Omizzolo, A., Gullieuszik, M., Bettoni, D., Moretti, A., Paccagnella, A., Jaffé, Y. L., Vulcani, B., Fritz, J., Couch, W., & D'Onofrio, M. 2016, *AJ*, 151, 78
- Pohlen, M. & Trujillo, I. 2006, *A&A*, 454, 759
- Quilis, V., Moore, B., & Bower, R. 2000, *Science*, 288, 1617
- Rettura, A., Rosati, P., Nonino, M., Fosbury, R. A. E., Gobat, R., Menci, N., Strazzullo, V., Mei, S., Demarco, R., & Ford, H. C. 2010, *ApJ*, 709, 512
- Roberts, I. D. & Parker, L. C. 2017, *MNRAS*, 467, 3268
- Roberts, I. D., Parker, L. C., & Karunakaran, A. 2016, *MNRAS*, 455, 3628
- Roediger, E. & Hensler, G. 2005, *A&A*, 433, 875
- Schawinski, K., Urry, C. M., Simmons, B. D., Fortson, L., Kaviraj, S., Keel, W. C., Lintott, C. J., Masters, K. L., Nichol, R. C., Sarzi, M., Skibba, R., Treister, E., Willett, K. W., Wong, O. I., & Yi, S. K. 2014, *MNRAS*, 440, 889
- Sérsic, J. L. 1968, *Atlas de Galaxias Australes*

Shen, S., Kauffmann, G., von der Linden, A., White, S. D. M., & Best, P. N. 2008, MNRAS, 389, 1074

Shen, S., Mo, H. J., White, S. D. M., Blanton, M. R., Kauffmann, G., Voges, W., Brinkmann, J., & Csabai, I. 2003, MNRAS, 343, 978

Shioya, Y., Bekki, K., Couch, W. J., & De Propris, R. 2002, ApJ, 565, 223

Simard, L., Mendel, J. T., Patton, D. R., Ellison, S. L., & McConnachie, A. W. 2011, ApJS, 196, 11

Simard, L., Willmer, C. N. A., Vogt, N. P., Sarajedini, V. L., Phillips, A. C., Weiner, B. J., Koo, D. C., Im, M., Illingworth, G. D., & Faber, S. M. 2002, ApJS, 142, 1

Smith, R., Fellhauer, M., & Assmann, P. 2012, MNRAS, 420, 1990

Tasca, L. A. M., Kneib, J.-P., Iovino, A., Le Fèvre, O., Kovač, K., Bolzonella, M., Lilly, S. J., Abraham, R. G., Cassata, P., Cucciati, O., Guzzo, L., Tresse, L., Zamorani, G., Capak, P., Garilli, B., Scodreggio, M., Sheth, K., Zucca, E., Carollo, C. M., Contini, T., Mainieri, V., Renzini, A., Bardelli, S., Bongiorno, A., Caputi, K., Coppa, G., de La Torre, S., de Ravel, L., Franzetti, P., Kampczyk, P., Knobel, C., Koekemoer, A. M., Lamareille, F., Le Borgne, J.-F., Le Brun, V., Maier, C., Mignoli, M., Pello, R., Peng, Y., Perez Montero, E., Ricciardelli, E., Silverman, J. D., Vergani, D., Tanaka, M., Abbas, U., Bottini, D., Cappi, A., Cimatti, A., Ilbert, O., Leauthaud, A., Maccagni, D., Marinoni, C., McCracken, H. J., Memeo, P., Meneux, B., Oesch, P., Porciani, C., Pozzetti, L., Scaramella, R., & Scarlata, C. 2009, A&A, 503, 379

Tinker, J. L. & Chen, H.-W. 2008, ApJ, 679, 1218

Tonnesen, S., Bryan, G. L., & van Gorkom, J. H. 2007, ApJ, 671, 1434

Toomre, A. & Toomre, J. 1972, *ApJ*, 178, 623

Trujillo, I., Conselice, C. J., Bundy, K., Cooper, M. C., Eisenhardt, P., & Ellis, R. S. 2007, *MNRAS*, 382, 109

Trujillo, I., Förster Schreiber, N. M., Rudnick, G., Barden, M., Franx, M., Rix, H.-W., Caldwell, J. A. R., McIntosh, D. H., Toft, S., Häussler, B., Zirm, A., van Dokkum, P. G., Labbé, I., Moorwood, A., Röttgering, H., van der Wel, A., van der Werf, P., & van Starckenburg, L. 2006, *ApJ*, 650, 18

Vaghmare, K., Barway, S., Mathur, S., & Kembhavi, A. K. 2015, *MNRAS*, 450, 873

Valentinuzzi, T., Fritz, J., Poggianti, B. M., Cava, A., Bettoni, D., Fasano, G., D’Onofrio, M., Couch, W. J., Dressler, A., Moles, M., Moretti, A., Omizzolo, A., Kjærgaard, P., Vanzella, E., & Varela, J. 2010, *ApJ*, 712, 226

van de Voort, F., Bahé, Y. M., Bower, R. G., Correa, C. A., Crain, R. A., Schaye, J., & Theuns, T. 2017, *MNRAS*, 466, 3460

van den Bosch, F. C., Aquino, D., Yang, X., Mo, H. J., Pasquali, A., McIntosh, D. H., Weinmann, S. M., & Kang, X. 2008, *MNRAS*, 387, 79

van Dokkum, P. G., Franx, M., Kriek, M., Holden, B., Illingworth, G. D., Magee, D., Bouwens, R., Marchesini, D., Quadri, R., Rudnick, G., Taylor, E. N., & Toft, S. 2008, *ApJ*, 677, L5

van Dokkum, P. G., Leja, J., Nelson, E. J., Patel, S., Skelton, R. E., Momcheva, I., Brammer, G., Whitaker, K. E., Lundgren, B., Fumagalli, M., Conroy, C., Förster Schreiber, N., Franx, M., Kriek, M., Labbé, I., Marchesini, D., Rix, H.-W., van der Wel, A., & Wuyts, S. 2013, *ApJ*, 771, L35

- Voges, W., Aschenbach, B., Boller, T., Bräuninger, H., Briel, U., Burkert, W., Dennerl, K., Englhauser, J., Gruber, R., Haberl, F., Hartner, G., Hasinger, G., Kürster, M., Pfeffermann, E., Pietsch, W., Predehl, P., Rosso, C., Schmitt, J. H. M. M., Trümper, J., & Zimmermann, H. U. 1999, *A&A*, 349, 389
- Wang, L., Yang, X., Shen, S., Mo, H. J., van den Bosch, F. C., Luo, W., Wang, Y., Lau, E. T., Wang, Q. D., Kang, X., & Li, R. 2014, *MNRAS*, 439, 611
- Wetzel, A. R., Cohn, J. D., & White, M. 2009a, *MNRAS*, 395, 1376
- . 2009b, *MNRAS*, 394, 2182
- Wetzel, A. R., Tinker, J. L., & Conroy, C. 2012, *MNRAS*, 424, 232
- White, M., Cohn, J. D., & Smit, R. 2010, *MNRAS*, 408, 1818
- Yagi, M., Komiyama, Y., Yoshida, M., Furusawa, H., Kashikawa, N., Koyama, Y., & Okamura, S. 2007, *ApJ*, 660, 1209
- Yang, X., Mo, H. J., van den Bosch, F. C., & Jing, Y. P. 2005, *MNRAS*, 356, 1293
- Yang, X., Mo, H. J., van den Bosch, F. C., Pasquali, A., Li, C., & Barden, M. 2007, *ApJ*, 671, 153
- Zabludoff, A. I. & Mulchaey, J. S. 1998, *ApJ*, 496, 39
- Zhang, B., Sun, M., Ji, L., Sarazin, C., Lin, X. B., Nulsen, P. E. J., Roediger, E., Donahue, M., Forman, W., Jones, C., Voit, G. M., & Kong, X. 2013, *ApJ*, 777, 122

Chapter 3

Further Observations of Disc Dependence on Environment

In the previous chapter, we discussed the dependence of disc scale length at fixed bulge mass on both field and group environments, characterized by X-ray brightness. We found in Fig. 2.6 that the disc scale lengths of low mass galaxies are preferentially truncated in XRS groups compared to XRW groups and the isolated field. In Chapter 2 we applied V_{max} weights to our data, and in this section we examine the results in Fig. 2.6 with no weights applied, since V_{max} weighting increases the impact of low mass galaxies and could shift disc scale lengths in our plots towards smaller values. To expand on our results in Fig. 2.9, which show that disc scale length versus bulge mass in our XRS, XRW, and isolated field samples has a very weak dependence on halo mass and group-centric distance (consistent with e.g. van den Bosch et al., 2008; Bamford et al., 2009; Zhang & Yang, 2017), we further investigate the dependence of stellar discs in our group samples on halo mass directly without factoring in X-ray brightness (as we have in our XRS and XRW subsets). In summary, in this section we further explore the dependence of disc truncation on X-ray brightness by plotting disc scale length versus bulge mass with no V_{max} weights, in bins of halo mass (rather than XRS and XRW), and also by visualizing our results by defining a parameter that describes X-ray luminosity at fixed halo mass.

To ensure that our results Fig. 2.6 are not influenced by our weighting scheme, we also plot disc scale length against bulge mass with no V_{max} weights applied to our data. Since we are performing a relative measurement between subsamples with the same redshift distribution, we do not expect our results to depend on the weights applied. In Fig. 3.1, we show that the disc truncation in group environments compared to the field is similar to Fig. 2.6, showing significant offsets between XRS, XRW and isolated field environments. Galaxies in XRW environments are slightly less truncated compared to the isolated field than in Fig. 2.6. We also note that the galaxies in in all three XRS, XRW, and isolated field samples are slightly larger on average than in Fig. 2.6, which is consistent with the fact that the applied weighting scheme increases the impact of low mass galaxies in Fig. 2.6. We emphasize that we are not focusing on determining individual galaxy sizes, since we are looking for systematic differences between our three samples. The relative differences between our three sample are upheld both with V_{max} weights in Fig. 2.6 and without them in Fig. 3.1.

Past studies have also shown that morphology at fixed stellar mass is only weakly dependent on measures of local density (such as halo mass) (e.g. Bamford et al., 2009; Huertas-Company et al., 2013). We saw evidence of weak environmental dependence on local density indicators in Fig. 2.8, which displayed no substantial differences in the disc truncation trends we found in Fig. 2.6 across bins of varying halo mass and group-centric radii, with the exception of an enhancement of disc truncation in the centres of cluster-sized halos. To confirm that the systematic differences we see in stellar disc truncation with respect to X-ray environment are not driven by halo mass, we sub-divided our total group sample into galaxies that are located in high and low mass halos (above and below the median halo mass $\log(M_h/M_\odot) = 14$, respectively), disregarding their X-ray properties. In Fig. 3.2 we show that disc scale lengths at low bulge mass are much smaller in group environments than in the field,

consistent with Fig. 2.6. However, looking at the difference between trends for large and small mass halos, we see that disc scale length only weakly depends on halo mass, where galaxies in large halos are only slightly more truncated than galaxies in small halos (consistent with Bamford et al., 2009). Disc truncation at low bulge mass in XRS groups compared to XRW groups is much stronger. These combined results show that disc properties depend more on X-ray brightness than on halo mass.

We will now describe another method of visualizing the dependence of disc scale length at fixed bulge mass on group X-ray luminosity. We define “X-ray strength” as the logarithmic difference of the X-ray luminosity of a galaxy group in the $L_x - M_{halo}$ plane at fixed halo mass, and the logarithmic value of the X-ray luminosity of the best-fit line shown in Fig. 2.2. Thus, positive values of X-ray strength correspond to galaxies in XRS groups in our discrete sample, while negative values correspond to galaxies in the XRW dataset. Fig. 3.3 shows X-ray strength as a function of halo mass, and labels our discrete samples from Fig. 2.2 for reference. Using X-ray strength as a variable, we can now create a continuous version of our results in Fig. 2.6. We show the continuous result in Fig. 3.4 for our subset of galaxies populating X-ray extremes, and we note that galaxies clustered at the low bulge mass end with smaller disc scale lengths systematically correspond to high values of X-ray strength. The stars overlaid on the individual galaxy datapoints show the binned R_d and $\log(M_{bulge}/M_\odot)$ averages and are coloured by average X-ray strength, and we notice that average X-ray strength appears to slowly decrease with increasing disc scale length and bulge mass. We note that our approach to discretize our datasets in Chapter 2 allows us to quantify differences between XRS and XRW samples in disc scale length, and we do not address the typical error in X-ray luminosity for the groups (which is of order 0.4 dex as given by Wang et al. (2014)) because both samples have the same systematics. Qualitatively, Fig. 2.6 and Fig. 3.4 are different visualizations of the same result.

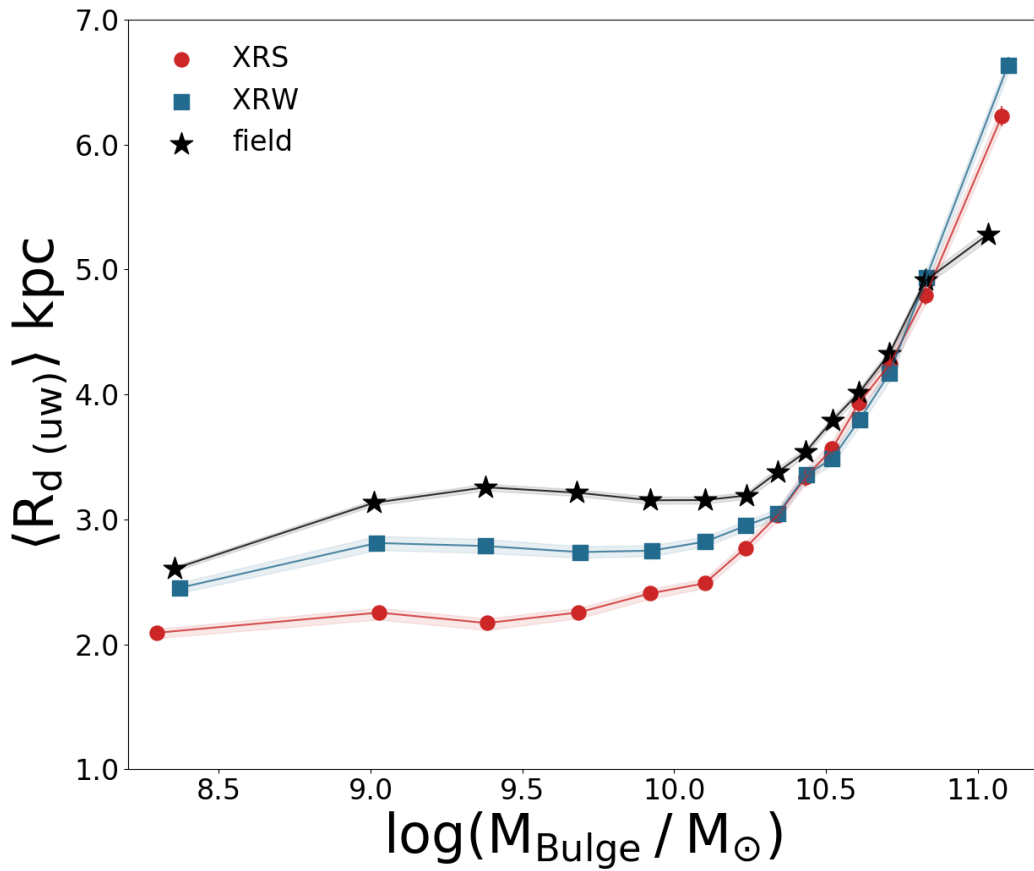


Figure 3.1 Exponential disc scale length versus bulge mass with no applied V_{max} weights. Shaded regions correspond to the standard error of the mean bin values.

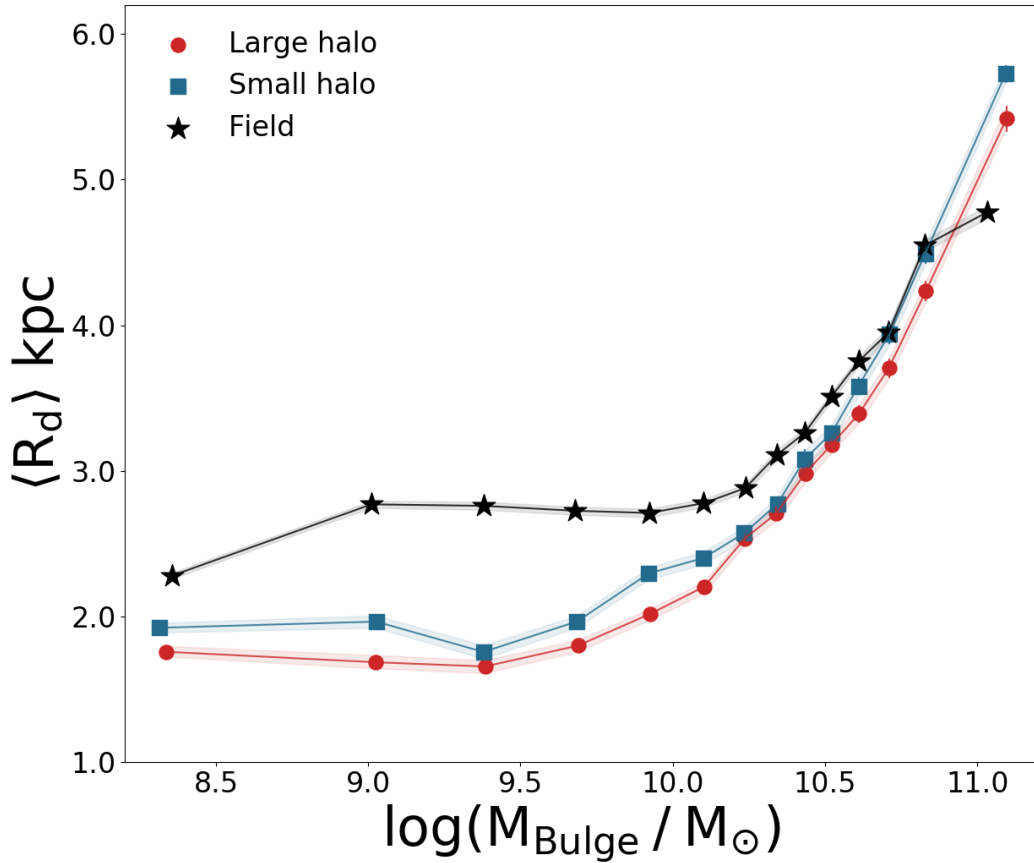


Figure 3.2 V_{max} weighted exponential disc scale length versus bulge mass, where environment corresponds to large halos in red (above $\log(M_h/M_{\odot}) = 14$), small halos in blue (below $\log(M_h/M_{\odot}) = 14$), and the isolated field sample in black. Error bars and shaded regions correspond to the standard error of the mean bin values.

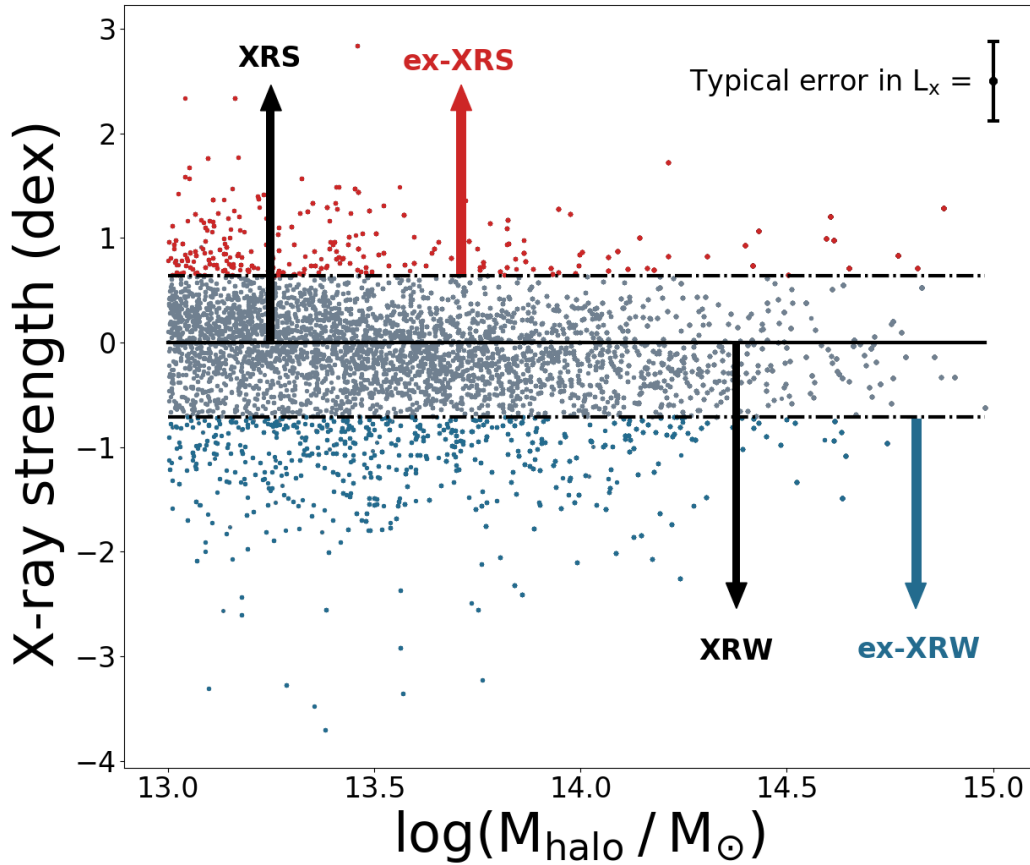


Figure 3.3 X-ray strength versus halo mass, where X-ray strength is defined as the difference between $\log(L_x)$ and the $\log(L_x)$ value from the best-fit relation in Fig. 2.2 at fixed halo mass $\log(M_h/M_\odot)$. Solid line at zero represents the line of best fit from which we defined our XRS and XRW samples, and dot-dashed lines represent the lines above and below which we defined the X-ray extremes in Fig. 2.2. For reference, the typical error in X-ray luminosity is shown, and corresponds to 0.4 dex as in Wang et al. (2014).

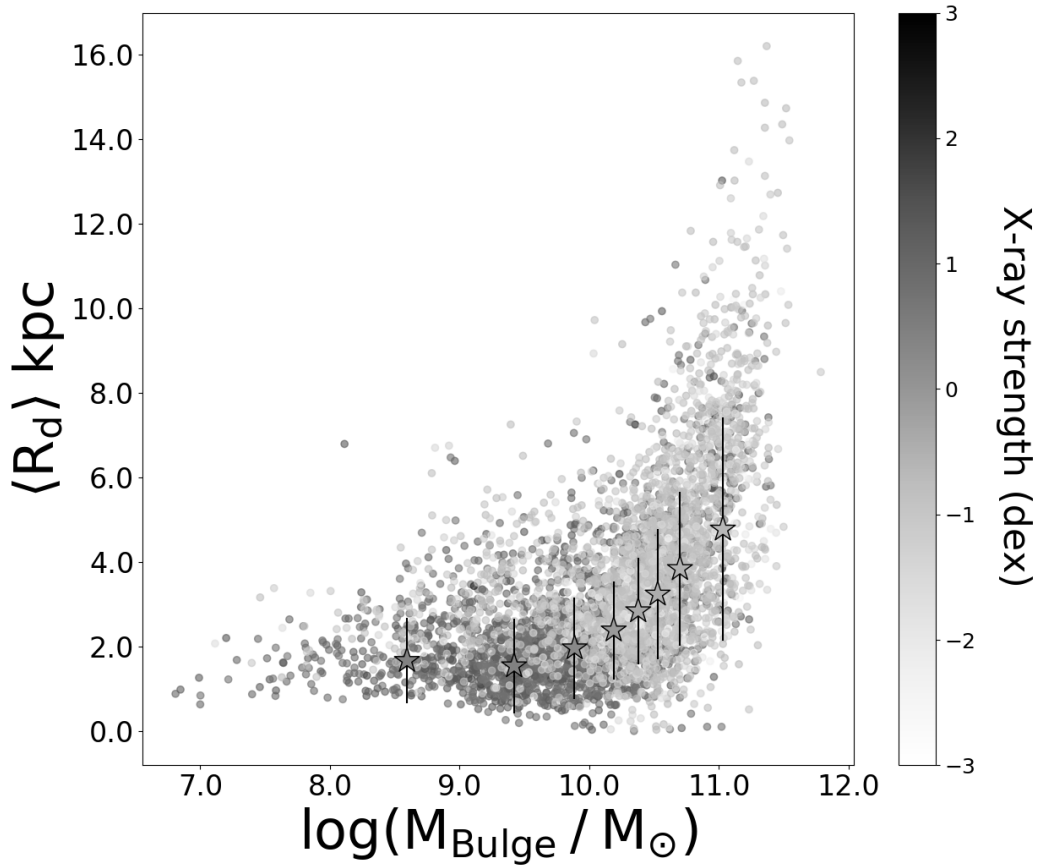


Figure 3.4 Exponential disc scale length versus bulge mass for X-ray extreme subsamples, where datapoints are coloured by the X-ray strength of the group environment (defined in Fig. 3.3). Stars outlined in black represent the V_{max} weighted average disc scale length and average bulge mass for a given bin, where the star colour corresponds to the average X-ray strength in a given bin. Black error bars correspond to standard deviation.

Bibliography

Bamford, S. P., Nichol, R. C., Baldry, I. K., Land, K., Lintott, C. J., Schawinski, K., Slosar, A., Szalay, A. S., Thomas, D., Tori, M., Andreescu, D., Edmondson, E. M., Miller, C. J., Murray, P., Raddick, M. J., & Vandenberg, J. 2009, MNRAS, 393, 1324

Huertas-Company, M., Mei, S., Shankar, F., Delaye, L., Raichoor, A., Covone, G., Finoguenov, A., Kneib, J. P., Le, F. O., & Povic, M. 2013, MNRAS, 428, 1715

van den Bosch, F. C., Aquino, D., Yang, X., Mo, H. J., Pasquali, A., McIntosh, D. H., Weinmann, S. M., & Kang, X. 2008, MNRAS, 387, 79

Wang, L., Yang, X., Shen, S., Mo, H. J., van den Bosch, F. C., Luo, W., Wang, Y., Lau, E. T., Wang, Q. D., Kang, X., & Li, R. 2014, MNRAS, 439, 611

Zhang, Y. & Yang, X. 2017, ArXiv e-prints

Chapter 4

Summary & Future Work

Galaxy evolution is a wide field of research that addresses how galaxy star-formation and morphological properties transform - both with environment, and over cosmic time. Overdense environments have been observed to quench star-formation (Lewis et al., 2002; Gómez et al., 2003; Balogh et al., 2004), and drive transformations of galaxy morphologies from disc to bulge-dominated (Oemler, 1974; Dressler, 1980; Postman & Geller, 1984; Goto et al., 2003; Blanton et al., 2005). Groups are intermediate environments that host galaxies with a wide range of morphologies (e.g. Eke et al., 2004), where we can study the mechanisms driving transformations in galaxy structure. Past studies have shown that the effective radii of high mass early-type galaxies are independent of environment (Pohlen & Trujillo, 2006; Maltby et al., 2010; Maltby et al., 2015), and the sizes of low mass disc-dominated galaxies are sensitive to environment (Tasca et al., 2009; Maltby et al., 2010; Peng et al., 2010). Additionally, since galaxy bulges at low-redshift do not experience growth in stellar mass (van Dokkum et al., 2013), it is logical to focus on disc dependencies with environment to address mechanisms that affect morphology (Hudson et al., 2010). For these reasons, we chose to focus solely on disc parameters obtained from bulge-disc decompositions in varied environments.

In Chapter 2, using a sample of SDSS galaxies from the Y07 group catalogue with X-ray properties from Wang et al. (2014) and structural parameters

from S11 and Mendel et al. (2014), we study the dependence of galaxy disc properties on environment. At low bulge mass, we find that galaxy discs are systematically smaller in group environments compared to the isolated field. We also show that galaxies are significantly truncated in X-ray rich (XRS) groups, as compared to galaxies in X-ray poor (XRW) groups (see Fig. 2.6). When comparing samples of galaxies sub-divided by morphological type (Sa/Sb and Sc/Sd), we see the same trends with disc scale lengths of field > XRW > XRS galaxies in both subsets (see Fig. 2.11). The dependence of disc scale length on X-ray environment becomes more significant in the extrema of our datasets, with discs in the most extreme X-ray bright environments being further truncated than the average trends (see Fig. 2.9). We also see evidence that star-forming discs (with $\log \text{SSFR} > -11 \text{ yr}^{-1}$) are larger than the average trends for the total sample (see Fig. 2.10), indicating that as discs are quenched, they are truncated from the outside-in. Our combined results are indicative of IGM density (traced by X-ray luminosity) being the culprit behind excess disc truncation in X-ray rich environments.

In Chapter 3, rather than discretizing our sample into subsets of XRS and XRW data as shown in Fig. 2.6, we visualize our main result in a continuous manner by defining an “X-ray strength” variable to quantify the X-ray environment (defined in Fig. 3.3). In Fig. 3.4, we show our continuous results for our X-ray extreme subsets of data, and emphasize that discs at fixed bulge mass in environments with higher X-ray strengths are systematically clustered at smaller disc scale lengths. Although, we note that the typical error in X-ray luminosity is of order 0.4 dex (as given by Wang et al., 2014), we find the same qualitative results that we showed using discrete datasets in Fig. 2.6. Additionally, in Fig. 3.2 we address the possible dependence of disc scale length at fixed bulge mass on halo mass. We discretize our dataset into “large halos” and “small halos” based on whether galaxies lie above or below the median halo mass of our group sample. For low mass galaxies, we show that galaxies

in groups are significantly truncated compared to galaxies in the isolated field (consistent with findings of Wetzel et al., 2012, at fixed stellar mass). We also find that galaxies in large halos are slightly smaller than galaxies in small halos. Although, we note that the dependence of morphology on halo mass in Fig. 3.2 is weaker than its dependence on X-ray environment in Fig. 2.6. Our results are consistent with previous findings that within groups, morphology only weakly depends on local density parameters (e.g. Bamford et al., 2009; Zhang & Yang, 2017). Our conclusions in Chapter 3 re-emphasize the importance of considering the effects of X-ray properties of groups and clusters on galaxy morphology, particularly for low mass galaxies.

In this thesis we suggest that the environmental mechanisms responsible for our results are possibly starvation and/or ram-pressure stripping. There are several methods that could be used to test which of these mechanisms may be causing our observational results. Starvation is thought to be a slow-acting quenching process that gradually causes a galaxy to use up its reservoirs of gas (from which it can form stars) (Larson et al., 1980; Bekki et al., 2002; van den Bosch et al., 2008), and causes discs to gradually “fade” from the outside-in. Previous work has shown that galaxies undergoing starvation will quench before morphological changes take place (Bekki et al., 2002; Boselli et al., 2006; Moran et al., 2006); meaning galaxy structure would remain relatively undisturbed over long timescales. In contrast, with ram-pressure stripping, the gas components of discs are very quickly stripped (Fujita & Nagashima, 1999; Quilis et al., 2000; Roediger & Hensler, 2005; Kapferer et al., 2009), and these findings from simulations are supported by radio observations of disturbed atomic hydrogen discs as galaxies travel through the IGM (e.g. Chung et al., 2007; Yagi et al., 2007; Zhang et al., 2013).

By extracting the radial extent of star-formation (traced by $H\alpha$) and comparing to stellar disc scale lengths, it is possible to quantify the physical disturbance of the star-forming disc compared to the stellar disc. To assess the

impacts of ram-pressure stripping on disc components, Abramson et al. (2011) conducts a multi-wavelength photometric study (including optical, $H\alpha$ and HI) of a galaxy undergoing active stripping in the Virgo Cluster. They find that the galaxy’s HI disc is radially truncated well-within the optical disc radius, with a large HI tail extending out of the plane of the disc (also see e.g. Chung et al., 2007). In addition, they find substantial $H\alpha$ emission outside of the midplane of the optical disc. The $H\alpha$ emission occurs because it is tracing young stars forming in gas from the galaxy’s interstellar medium (ISM) that was displaced out of the plane of the disc by ram-pressure. They conclude that the $H\alpha$ emission outside of the disc midplane (called “the upturn”) could be used as a diagnostic of active ram-pressure stripping. Identifying the upturn in $H\alpha$ could distinguish ram-pressure stripping from the effects of starvation, which would not violently push the ISM out of the galaxy, and therefore would not display an upturn in $H\alpha$. Additionally, Finn et al. (2018) probe the size of the star-forming disc with $24\mu\text{m}$ imaging to compare to the optical disc and show that galaxies in overdense environments have more centrally concentrated star-formation. These multi-wavelength studies are a promising avenue for investigating environmental effects on galaxy discs.

To detect the physical extent of star-formation in a disc, we can also use Integrated Field Unit (IFU) surveys. IFU surveys such as the Calar Alto Legacy Integral Field Area survey (CALIFA; Sánchez et al., 2012), the Mapping nearby Galaxies at Apache Point Observatory survey (MaNGA; Bundy et al., 2015), and the SAMI Galaxy Survey (SAMI; Green et al., 2018) have been developed to provide spatially resolved galaxy spectra across a two-dimensional field of view. Since IFU spectroscopy can map spectral features across the face of a galaxy, it is possible to extract the physical extent of the star-forming radius from $H\alpha$ emission. Our research group has begun to trace the radial extent of $H\alpha$ emission using MaNGA galaxies, where star-forming radii were mea-



Figure 4.1 Optical image of galaxy SDSS galaxy include in MaNGA survey, SDSS ID: J162457.27+393152.4. Image credit: SDSS.

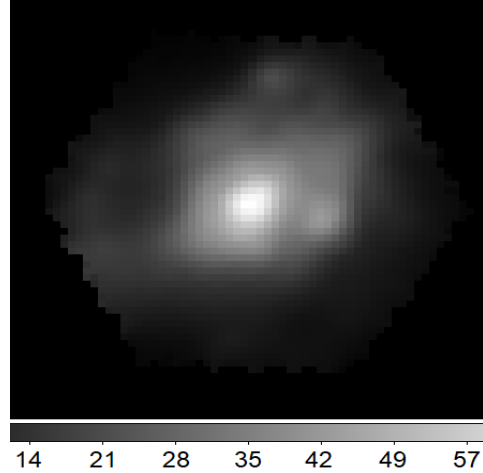


Figure 4.2 H α map created with MaNGA datacube. Colourbar represents the sum of H α flux in units of 10^{-17} erg/s/cm 2 /Å/spaxel. Image credit: Rachel Brown.

sured by applying an exponentially declining surface brightness profile fit (see Eqn. 2.4) to galaxy H α maps (see Fig. 4.2).

Another method that could be used to ascertain whether ram-pressure stripping or starvation is the dominant process causing galaxy disc truncation is to observe intracluster light (ICL). The origin of the diffuse ICL in galaxy clusters has been linked to stripped material and stars from tidal interactions, during the process of hierarchical assembly (Vílchez-Gómez, 1999; Mihos et al., 2005). Additionally, ram-pressure stripping is thought to contribute to ICL (Verdugo et al., 2015), since galaxies undergoing ram-pressure stripping can have HI tails that extend as far as 100 kpc with young stars forming in-situ within them (Kenney et al., 2008). Thus, an enhancement in ICL could be indicative of ram-pressure stripping. By comparison, we stipulate that starvation would not cause an enhancement in ICL, since it would not cause stars or gas to be violently removed from galaxies. An interesting follow-up would be to measure ICL in galaxy groups from our sample, to test

whether ICL would be enhanced in XRS systems. We might expect that XRS groups would have higher ICL contributions than XRW groups, because the XRS groups trace higher IGM densities, which would cause more substantial ram-pressure stripping effects. Although, the ICL is very faint (of order 25 - 26 mag/arcsec² in a red filter) making it difficult to measure. To study the ICL, deep optical imaging is required (Vílchez-Gómez, 1999; Feldmeier et al., 2002).

This thesis has examined the dependence of galaxy disc structural parameters on environment, characterized by X-ray luminosity. We have shown that the discs of low mass galaxies are truncated in X-ray rich group environments, as compared to X-ray poor groups, and in the isolated field. Our work highlights the importance of considering X-ray brightness as an environmental metric, and motivates further studies of galaxy bulge and disc components and their dependence on environment. Multiple IFU data releases combined with innovative ideas such as applying bulge-disc decompositions directly to IFU datacubes (Johnston et al., 2017) will allow the continued exploration of the transformation of galaxy disc morphology with environment in future work.

Bibliography

- Abramson, A., Kenney, J. D. P., Crowl, H. H., Chung, A., van Gorkom, J. H., Vollmer, B., & Schiminovich, D. 2011, *AJ*, 141, 164
- Balogh, M. L., Baldry, I. K., Nichol, R., Miller, C., Bower, R., & Glazebrook, K. 2004, *ApJ*, 615, L101
- Bamford, S. P., Nichol, R. C., Baldry, I. K., Land, K., Lintott, C. J., Schawinski, K., Slosar, A., Szalay, A. S., Thomas, D., Torri, M., Andreescu, D., Edmondson, E. M., Miller, C. J., Murray, P., Raddick, M. J., & Vandenberg, J. 2009, *MNRAS*, 393, 1324
- Bekki, K., Couch, W. J., & Shioya, Y. 2002, *ApJ*, 577, 651
- Blanton, M. R., Eisenstein, D., Hogg, D. W., Schlegel, D. J., & Brinkmann, J. 2005, *ApJ*, 629, 143
- Boselli, A., Boissier, S., Cortese, L., Gil de Paz, A., Seibert, M., Madore, B. F., Buat, V., & Martin, D. C. 2006, *ApJ*, 651, 811
- Bundy, K., Bershady, M. A., Law, D. R., Yan, R., Drory, N., MacDonald, N., Wake, D. A., Cherinka, B., Sánchez-Gallego, J. R., Weijmans, A.-M., Thomas, D., Tremonti, C., Masters, K., Coccato, L., Diamond-Stanic, A. M., Aragón-Salamanca, A., Avila-Reese, V., Badenes, C., Falcón-Barroso, J., Belfiore, F., Bizyaev, D., Blanc, G. A., Bland-Hawthorn, J., Blanton, M. R., Brownstein, J. R., Byler, N., Cappellari, M., Conroy, C., Dutton, A. A., Em-sellem, E., Etherington, J., Frinchaboy, P. M., Fu, H., Gunn, J. E., Harding, P., Johnston, E. J., Kauffmann, G., Kinemuchi, K., Klaene, M. A., Knapen, J. H., Leauthaud, A., Li, C., Lin, L., Maiolino, R., Malanushenko,

- V., Malanushenko, E., Mao, S., Maraston, C., McDermid, R. M., Merri-
field, M. R., Nichol, R. C., Oravetz, D., Pan, K., Parejko, J. K., Sanchez,
S. F., Schlegel, D., Simmons, A., Steele, O., Steinmetz, M., Thanjavur, K.,
Thompson, B. A., Tinker, J. L., van den Bosch, R. C. E., Westfall, K. B.,
Wilkinson, D., Wright, S., Xiao, T., & Zhang, K. 2015, *ApJ*, 798, 7
- Chung, A., van Gorkom, J. H., Kenney, J. D. P., & Vollmer, B. 2007, *ApJ*,
659, L115
- Dressler, A. 1980, *ApJ*, 236, 351
- Eke, V. R., Baugh, C. M., Cole, S., Frenk, C. S., Norberg, P., Peacock, J. A.,
Baldry, I. K., Bland-Hawthorn, J., Bridges, T., Cannon, R., Colless, M.,
Collins, C., Couch, W., Dalton, G., de Propriis, R., Driver, S. P., Efstathiou,
G., Ellis, R. S., Glazebrook, K., Jackson, C., Lahav, O., Lewis, I., Lumsden,
S., Maddox, S., Madgwick, D., Peterson, B. A., Sutherland, W., & Taylor,
K. 2004, *MNRAS*, 348, 866
- Feldmeier, J. J., Mihos, J. C., Morrison, H. L., Rodney, S. A., & Harding, P.
2002, *ApJ*, 575, 779
- Finn, R. A., Desai, V., Rudnick, G., Balogh, M., Haynes, M. P., Jablonka, P.,
Koopmann, R. A., Moustakas, J., Peng, C. Y., Poggianti, B., Rines, K., &
Zaritsky, D. 2018, *ApJ*, 862, 149
- Fujita, Y. & Nagashima, M. 1999, *ApJ*, 516, 619
- Gómez, P. L., Nichol, R. C., Miller, C. J., Balogh, M. L., Goto, T., Zabludoff,
A. I., Romer, A. K., Bernardi, M., Sheth, R., Hopkins, A. M., Castander,
F. J., Connolly, A. J., Schneider, D. P., Brinkmann, J., Lamb, D. Q., Sub-
baRao, M., & York, D. G. 2003, *ApJ*, 584, 210
- Goto, T., Yamauchi, C., Fujita, Y., Okamura, S., Sekiguchi, M., Smail, I.,
Bernardi, M., & Gomez, P. L. 2003, *MNRAS*, 346, 601

Green, A. W., Croom, S. M., Scott, N., Cortese, L., Medling, A. M., D'Eugenio, F., Bryant, J. J., Bland-Hawthorn, J., Allen, J. T., Sharp, R., Ho, I.-T., Groves, B., Drinkwater, M. J., Mannering, E., Harischandra, L., van de Sande, J., Thomas, A. D., O'Toole, S., McDermid, R. M., Vuong, M., Sealey, K., Bauer, A. E., Brough, S., Catinella, B., Cecil, G., Colless, M., Couch, W. J., Driver, S. P., Federrath, C., Foster, C., Goodwin, M., Hampton, E. J., Hopkins, A. M., Jones, D. H., Konstantopoulos, I. S., Lawrence, J. S., Leon-Saval, S. G., Liske, J., López-Sánchez, Á. R., Lorente, N. P. F., Mould, J., Obreschkow, D., Owers, M. S., Richards, S. N., Robotham, A. S. G., Schaefer, A. L., Sweet, S. M., Taranu, D. S., Tescari, E., Tonini, C., & Zafar, T. 2018, *MNRAS*, 475, 716

Hudson, M. J., Stevenson, J. B., Smith, R. J., Wegner, G. A., Lucey, J. R., & Simard, L. 2010, *MNRAS*, 409, 405

Johnston, E. J., Häußler, B., Aragón-Salamanca, A., Merrifield, M. R., Bamford, S., Bershady, M. A., Bundy, K., Drory, N., Fu, H., Law, D., Nitschelm, C., Thomas, D., Roman Lopes, A., Wake, D., & Yan, R. 2017, *MNRAS*, 465, 2317

Kapferer, W., Sluka, C., Schindler, S., Ferrari, C., & Ziegler, B. 2009, *A&A*, 499, 87

Kenney, J. D. P., Tal, T., Crowl, H. H., Feldmeier, J., & Jacoby, G. H. 2008, *ApJ*, 687, L69

Larson, R. B., Tinsley, B. M., & Caldwell, C. N. 1980, *ApJ*, 237, 692

Lewis, I., Balogh, M., De Propriis, R., Couch, W., Bower, R., Offer, A., Bland-Hawthorn, J., Baldry, I. K., Baugh, C., Bridges, T., Cannon, R., Cole, S., Colless, M., Collins, C., Cross, N., Dalton, G., Driver, S. P., Efstathiou, G., Ellis, R. S., Frenk, C. S., Glazebrook, K., Hawkins, E., Jackson, C., Lahav,

- O., Lumsden, S., Maddox, S., Madgwick, D., Norberg, P., Peacock, J. A., Percival, W., Peterson, B. A., Sutherland, W., & Taylor, K. 2002, *MNRAS*, 334, 673
- Maltby, D. T., Aragón-Salamanca, A., Gray, M. E., Barden, M., Häußler, B., Wolf, C., Peng, C. Y., Jahnke, K., McIntosh, D. H., Böhm, A., & van Kampen, E. 2010, *MNRAS*, 402, 282
- Maltby, D. T., Aragón-Salamanca, A., Gray, M. E., Hoyos, C., Wolf, C., Jogee, S., & Böhm, A. 2015, *Monthly Notices of the Royal Astronomical Society*, 447, 1506
- Mendel, J. T., Simard, L., Palmer, M., Ellison, S. L., & Patton, D. R. 2014, *ApJS*, 210, 3
- Mihos, J. C., Harding, P., Feldmeier, J., & Morrison, H. 2005, *ApJ*, 631, L41
- Moran, S. M., Ellis, R. S., Treu, T., Salim, S., Rich, R. M., Smith, G. P., & Kneib, J.-P. 2006, *ApJ*, 641, L97
- Oemler, Jr., A. 1974, *ApJ*, 194, 1
- Peng, Y.-j., Lilly, S. J., Kovač, K., Bolzonella, M., Pozzetti, L., Renzini, A., Zamorani, G., Ilbert, O., Knobel, C., Iovino, A., Maier, C., Cucciati, O., Tasca, L., Carollo, C. M., Silverman, J., Kampczyk, P., de Ravel, L., Sanders, D., Scoville, N., Contini, T., Mainieri, V., Scodreggio, M., Kneib, J.-P., Le Fèvre, O., Bardelli, S., Bongiorno, A., Caputi, K., Coppa, G., de la Torre, S., Franzetti, P., Garilli, B., Lamareille, F., Le Borgne, J.-F., Le Brun, V., Mignoli, M., Perez Montero, E., Pello, R., Ricciardelli, E., Tanaka, M., Tresse, L., Vergani, D., Welikala, N., Zucca, E., Oesch, P., Abbas, U., Barnes, L., Bordoloi, R., Bottini, D., Cappi, A., Cassata, P., Cimatti, A., Fumana, M., Hasinger, G., Koekemoer, A., Leauthaud, A., Maccagni, D.,

- Marinoni, C., McCracken, H., Memeo, P., Meneux, B., Nair, P., Porciani, C., Presotto, V., & Scaramella, R. 2010, *ApJ*, 721, 193
- Pohlen, M. & Trujillo, I. 2006, *A&A*, 454, 759
- Postman, M. & Geller, M. J. 1984, *ApJ*, 281, 95
- Quilis, V., Moore, B., & Bower, R. 2000, *Science*, 288, 1617
- Roediger, E. & Hensler, G. 2005, *A&A*, 433, 875
- Sánchez, S. F., Kennicutt, R. C., Gil de Paz, A., van de Ven, G., Vílchez, J. M., Wisotzki, L., Walcher, C. J., Mast, D., Aguerri, J. A. L., Albiol-Pérez, S., Alonso-Herrero, A., Alves, J., Bakos, J., Bartáková, T., Bland-Hawthorn, J., Boselli, A., Bomans, D. J., Castillo-Morales, A., Cortijo-Ferrero, C., de Lorenzo-Cáceres, A., Del Olmo, A., Dettmar, R.-J., Díaz, A., Ellis, S., Falcón-Barroso, J., Flores, H., Gallazzi, A., García-Lorenzo, B., González Delgado, R., Gruel, N., Haines, T., Hao, C., Husemann, B., Iglésias-Páramo, J., Jahnke, K., Johnson, B., Jungwiert, B., Kalinova, V., Kehrig, C., Kupko, D., López-Sánchez, Á. R., Lyubenova, M., Marino, R. A., Mármol-Queraltó, E., Márquez, I., Masegosa, J., Meidt, S., Mendez-Abreu, J., Monreal-Ibero, A., Montijo, C., Mourão, A. M., Palacios-Navarro, G., Papaderos, P., Pasquali, A., Peletier, R., Pérez, E., Pérez, I., Quirrenbach, A., Relaño, M., Rosales-Ortega, F. F., Roth, M. M., Ruiz-Lara, T., Sánchez-Blázquez, P., Sengupta, C., Singh, R., Stanishev, V., Trager, S. C., Vazdekis, A., Viironen, K., Wild, V., Zibetti, S., & Ziegler, B. 2012, *A&A*, 538, A8
- Simard, L., Mendel, J. T., Patton, D. R., Ellison, S. L., & McConnachie, A. W. 2011, *ApJS*, 196, 11
- Tasca, L. A. M., Kneib, J.-P., Iovino, A., Le Fèvre, O., Kovač, K., Bolzonella, M., Lilly, S. J., Abraham, R. G., Cassata, P., Cucciati, O., Guzzo, L., Tresse, L., Zamorani, G., Capak, P., Garilli, B., Scodreggio, M., Sheth, K., Zucca, E.,

- Carollo, C. M., Contini, T., Mainieri, V., Renzini, A., Bardelli, S., Bongiorno, A., Caputi, K., Coppa, G., de La Torre, S., de Ravel, L., Franzetti, P., Kampczyk, P., Knobel, C., Koekemoer, A. M., Lamareille, F., Le Borgne, J.-F., Le Brun, V., Maier, C., Mignoli, M., Pello, R., Peng, Y., Perez Montero, E., Ricciardelli, E., Silverman, J. D., Vergani, D., Tanaka, M., Abbas, U., Bottini, D., Cappi, A., Cimatti, A., Ilbert, O., Leauthaud, A., Maccagni, D., Marinoni, C., McCracken, H. J., Memeo, P., Meneux, B., Oesch, P., Porciani, C., Pozzetti, L., Scaramella, R., & Scarlata, C. 2009, *A&A*, 503, 379
- van den Bosch, F. C., Aquino, D., Yang, X., Mo, H. J., Pasquali, A., McIntosh, D. H., Weinmann, S. M., & Kang, X. 2008, *MNRAS*, 387, 79
- van Dokkum, P. G., Leja, J., Nelson, E. J., Patel, S., Skelton, R. E., Momcheva, I., Brammer, G., Whitaker, K. E., Lundgren, B., Fumagalli, M., Conroy, C., Förster Schreiber, N., Franx, M., Kriek, M., Labbé, I., Marchesini, D., Rix, H.-W., van der Wel, A., & Wuyts, S. 2013, *ApJ*, 771, L35
- Verdugo, C., Combes, F., Dasyra, K., Salomé, P., & Braine, J. 2015, *A&A*, 582, A6
- Vílchez-Gómez, R. 1999, in *Astronomical Society of the Pacific Conference Series*, Vol. 170, *The Low Surface Brightness Universe*, ed. J. I. Davies, C. Impey, & S. Phillips, 349
- Wang, L., Yang, X., Shen, S., Mo, H. J., van den Bosch, F. C., Luo, W., Wang, Y., Lau, E. T., Wang, Q. D., Kang, X., & Li, R. 2014, *MNRAS*, 439, 611
- Wetzell, A. R., Tinker, J. L., & Conroy, C. 2012, *MNRAS*, 424, 232
- Yagi, M., Komiyama, Y., Yoshida, M., Furusawa, H., Kashikawa, N., Koyama, Y., & Okamura, S. 2007, *ApJ*, 660, 1209

Yang, X., Mo, H. J., van den Bosch, F. C., Pasquali, A., Li, C., & Barden, M. 2007, *ApJ*, 671, 153

Zhang, B., Sun, M., Ji, L., Sarazin, C., Lin, X. B., Nulsen, P. E. J., Roediger, E., Donahue, M., Forman, W., Jones, C., Voit, G. M., & Kong, X. 2013, *ApJ*, 777, 122

Zhang, Y. & Yang, X. 2017, ArXiv e-prints

This page intentionally left blank.